



Estimating the effect of assumed initial damage to the hydraulic stability of pattern-placed revetments on dikes using finite element modeling

N. van der Vegt^{a,b}, W.J. Klerk^{a,c,*}, D.J. Peters^a, M.R.A. van Gent^{a,d}, B. Hofland^a

^a Delft University of Technology, P.O. Box 5048, Delft, 2600 GA, The Netherlands

^b HKV Consultants, Botter 11-29, 8232 JN, Lelystad, The Netherlands

^c Department of Flood Risk Management, Deltares, P.O. Box 177, 2600 MH, Delft, The Netherlands

^d Department of Hydraulic Engineering, Deltares, P.O. Box 177, 2600 MH, Delft, The Netherlands

ARTICLE INFO

Dataset link: https://github.com/nielsvandervegt/fem_patternplacedrevetment

Keywords:

Flood defenses
Dikes
Risk-based maintenance
Pattern-placed revetment
Wave impact
Finite element modeling
Surrogate modeling
Reliability analysis
Vulnerability

ABSTRACT

Initial damage, caused by previous wave loading or other events, might affect the hydraulic stability of pattern-placed revetments. Three common types of damage are considered in this study. The effect of this assumed initial damage on the hydraulic stability and failure probability of revetments is quantified using a FEM model. This model is developed using data from large-scale flume and field experiments. Using results from the FEM model, surrogate models are created to predict the effect of each type of initial damage on the hydraulic stability and failure probability. Through the use of these surrogate models, it is demonstrated that S-shaped deformation caused by filter migration around the wave impact zone has the largest effect on the hydraulic stability decreasing up to 30%, and failure probability per year increasing up to 10,000 times. When the granular filling between the joints of the columns is washed-out, the stability decreases up to 29% and the failure probability increases up to 700 times. A missing column has a limited effect on the hydraulic stability and failure probability when there is no other (structural) damage. However, if it originates from underlying damage, it might be an initial sign of total failure of the revetment. This study demonstrates the effectiveness of finite element modeling for studying (damaged) revetments, which can be used to complement flume experiments. The results can be used to prioritize maintenance efforts in risk-based maintenance of pattern-placed revetments.

1. Introduction

Flood defenses, such as dikes, are located worldwide, serving the common purpose of mitigating the risk of flooding. Over time, a flood defense will incur damage, leading to an increased risk of flooding. To ensure that flood defense stays in optimal condition, risk-based maintenance can be applied. This maintenance strategy aims to prioritize maintenance efforts based on the potential risks and consequences associated with the deteriorating conditions incurred by damage (Klerk, 2022). To effectively apply risk-based maintenance, understanding the actual condition of the flood defense, and the effects of damage to the performance of the flood defense is crucial.

In this paper, we focus on the effect of damage on the hydraulic stability of dike revetments made of pattern-placed elements, hereafter: pattern-placed revetments. These revetments are typically positioned in the wave impact zone and are designed to protect the dike from wave loading (Pilarczyk et al., 1995). Since the 1980s, extensive research

has been conducted to investigate the hydraulic stability of these revetments. Experiments have been conducted in large-scale flume facilities like the Delta flume (Burger, 1983; Bezuijen, 1984; Wouters, 1993; Lubbers and Klein Breteler, 2000) and the Großer Wellenkanal (Gier et al., 2012), offering controlled environments for studying the hydraulic stability of such revetments under wave loading. The outcomes of these experiments have led to the proposal of various stability models (Pilarczyk et al., 1995; Klein Breteler, 1995; Flikweert, 2003; Peters, 2017). These models commonly incorporate parameters such as wave height, Iribarren number, leakage length, and an empiric damage parameter to describe and predict the hydraulic stability of pattern-placed revetments subjected to wave loading.

Between 2003 and 2007 a research program was initiated to reinforce dikes in the province of Zeeland, the Netherlands (Flikweert and Akkerman, 2005). Part of this program involved several experiments on pattern-placed revetments in the field (Coeveld, 2003a; Peters, 2007)

* Corresponding author at: Delft University of Technology, P.O. Box 5048, Delft, 2600 GA, The Netherlands.

E-mail addresses: N.vanderVegt@hkv.nl (N. van der Vegt), WouterJan.Klerk@deltares.nl (W.J. Klerk), D.J.Peters@tudelft.nl (D.J. Peters), Marcel.vanGent@deltares.nl (M.R.A. van Gent), B.Hofland@tudelft.nl (B. Hofland).

<https://doi.org/10.1016/j.coastaleng.2024.104484>

Received 25 August 2023; Received in revised form 26 January 2024; Accepted 5 February 2024

Available online 7 February 2024

0378-3839/© 2024 The Author(s). Published by Elsevier B.V. This is an open access article under the CC BY license (<http://creativecommons.org/licenses/by/4.0/>).

and the Delta flume (Eysink and Klein Breteler, 2003; Coeveld et al., 2005; Klein Breteler and Eysink, 2007), resulting in the development of new models and insights (Coeveld, 2003b; Klein Breteler, 2007). As part of this program, an empirical model named ‘SteenToets’ was created to evaluate the hydraulic stability of pattern-placed revetments based on newly developed knowledge (Klein Breteler and Mourik, 2009).

The majority of earlier mentioned studies have predominantly focused on intact revetments, leaving the effects of damage on the hydraulic stability relatively unknown or reliant on expert judgment. In particular, only two experiments have been conducted on intentionally damaged pattern-placed revetments in the past 30 years (De Vroeg, 1992; Coeveld et al., 2005; Klein Breteler and Eysink, 2007). While some models, such as the latest version of SteenToets (Klein Breteler and Mourik, 2019), can evaluate the hydraulic stability of damaged revetments (e.g. without joint-filling or with a loose element), they often rely on conservative assumptions or expert opinions for corrections.

In 2017 risk-based safety standards for flood defences were introduced in the Netherlands. These provide a basis for risk-based maintenance, but this requires knowledge on the effect of damage on the hydraulic stability. Also, Klerk et al. (2021) showed that only a limited number of damages to revetments were identified in visual inspections, and it is hypothesized that this is amongst others due to the large number of different damage types inspectors have to look for. Knowledge on the effect of damage will thus not only enable applying the right maintenance measures, but can also be used as basis for more targeted and efficient inspections aimed at identifying the most crucial types of damage.

In this paper, we present a methodology and model using finite element modeling (FEM model) aimed at assessing the effect of damage on the hydraulic stability of pattern-placed revetment. Finite element modeling has previously proven successful in analyzing the static equilibrium of pattern-placed revetments subjected to wave loading (Bezuijen et al., 1990; Frissen et al., 2002), making it a viable and cheaper alternative to experimental studies. We applied the FEM model and methodology to study three common types of damage: deformation, washed-out joint filling, and a missing element. For each type of damage, a surrogate model is derived from the output of the FEM model

to quantify its effect on the hydraulic stability and failure probability of a pattern-placed revetment. This paper addresses two key questions:

- (1) What are the primary factors leading to a reduction in the hydraulic stability of a pattern-placed revetment?
- (2) How does damage affect the hydraulic stability and failure probability of a pattern-placed revetment?

The structure of this paper is organized as follows: Section 2 introduces the methodology and describes the development of the FEM model. In Section 3, surrogate models are derived and analyses are conducted to quantify the effect of the three types of damage on hydraulic stability and failure probability. Section 4 provides a discussion of the results, and finally, Section 5 summarizes the conclusions and recommendations.

2. Methodology and model development

An integral aspect of this study involves the development of a FEM model capable of simulating the dynamic behavior of damaged pattern-placed revetments under wave loading. The details of the development of this model are described in Section 2.1. Given the impracticality of directly applying the FEM model within analyses, surrogate models are derived on the output. This approach is described in Section 2.2. Finally, the effect of damage on the hydraulic stability and failure probability is studied using surrogate models. The approach for both analyses is described in Section 2.3. Fig. 1 shows a flow chart that illustrates these three steps.

2.1. Finite element modeling of (damaged) revetments

Because wave impacts are highly dynamic events, a finite element software suite capable of solving a dynamic equilibrium is required. In our study, we opted for ‘Abaqus Explicit 2019’ to develop the FEM model. Next to its explicit dynamic solver, the software suite offers a Python API which we used to fully automate the model generation. This is beneficial as it allows us to create a script to generate a FEM model based on a few input parameters. In the following paragraphs, we delve into the specifics of the development of the FEM model.

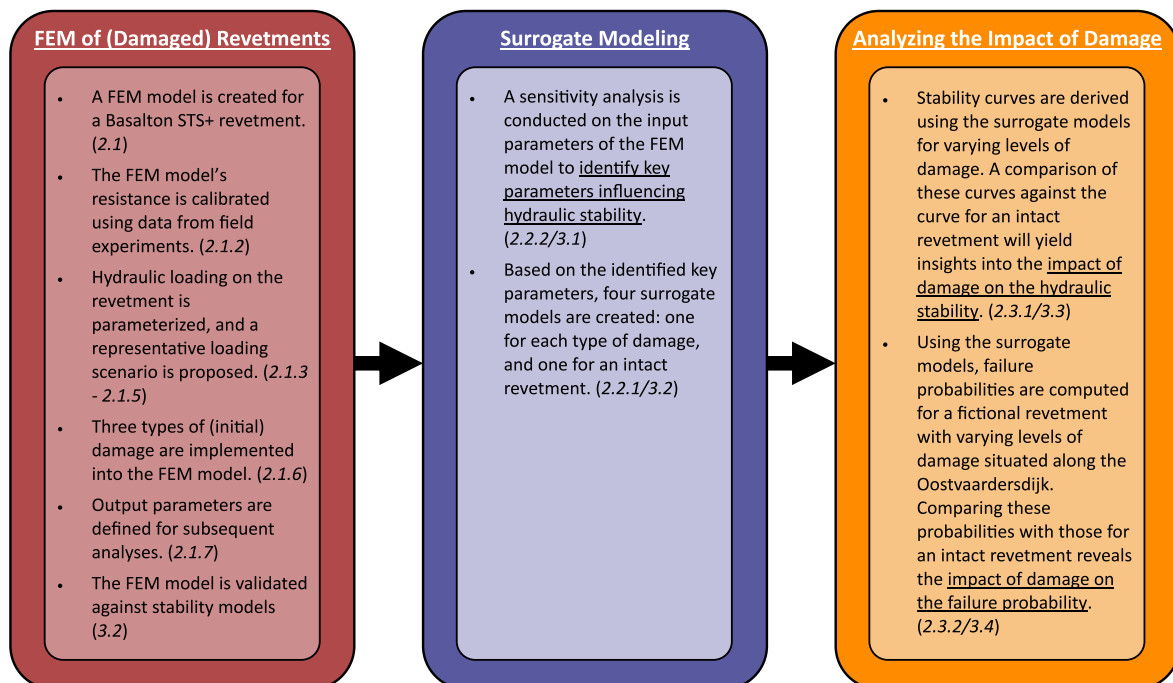


Fig. 1. Flow chart illustrating the connection between the model development, methodology, and results, with corresponding section numbers indicated in italics.

2.1.1. Modeling the revetment geometry

Pattern-placed revetments consist of various components, like the top layer, the filter layer, and the filling between the elements (referred to as joint filling). The top layer is the most important component, typically composed of arranged elements made of natural stone or concrete. These elements can be broadly classified as blocks or columns. While blocks are rectangular and tightly arranged, columns are irregular. The open spaces between the columns are typically filled with joint filling to enhance clamping. Also, in accordance with their name, columns generally have a larger height-over-width ratio than blocks, which is beneficial for their stability (Peters, 2017).

In our study, we focus on a top layer of Basalton® STS+ columns (Holcim Coastal, 2018), a commonly used top layer in the Netherlands. One set of this top layer consists of eighteen unique concrete columns and spans an area of 1.09 by 1.20 m. Within the FEM model, we model three sets along the slope (B_m) with a top layer thickness (D) of 0.3 m, as illustrated in Fig. 2. The surface below the columns, as well as the toe, are modeled as rigid surfaces.

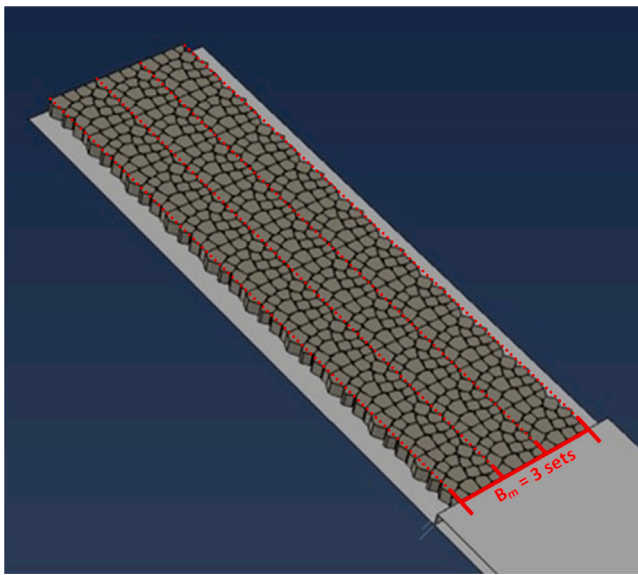


Fig. 2. Geometry of a pattern-placed revetment on a slope in the FEM model.

The columns themselves are modeled as a deformable body, utilizing a linear elastic model to represent the normal force between the columns. The material properties assigned to the columns align with typical concrete standards (Blok, 2014): Young's modulus (E_c) of 50 GPa, a Poisson ratio (ν_c) of 0.2, and a density ($\rho_{c,sub}$) set to 1275 kN/m³, representing the submerged density of concrete in saltwater. The columns situated at the outer edge of the model are constrained in translation and rotation over some axes, mimicking conditions similar to being adjacent to a wall or other columns.

In reality, both the filter layer and joint filling consist of granular material. Physically modeling the filter layer and joint filling in the FEM model would increase its complexity and significantly prolong the simulation time. Experimenting with modeling joint filling as deformable bodies led to a thirty-fold increase in simulation time. Due to this considerable time increase, we opt for a mathematical model to calculate the filter response based on the properties of the filter layer and joint filling, as described in Section 2.1.3.

The interaction between the columns themselves and the underlying surface (filter layer) is modeled as tangential behavior. This approach allows for the accurate representation of the complex frictional forces acting between the columns and the filter layer caused by the wave loading. The friction coefficient between the columns and the filter layer (μ_f) is set to 0.6, based on experiments conducted

by Schoen (2004). Furthermore, the friction coefficient between the columns themselves (μ_c) varies depending on the amount of joint filling and subsequent clamping between the columns. Because the joint filling is not physically modeled, this coefficient is calibrated as discussed in Section 2.1.2.

2.1.2. Calibration of revetment resistance

The joint filling between the columns provides additional clamping. Because joint filling is not physically modeled in the FEM model, the hydraulic stability of the revetment is underestimated. To account for this, we calibrated the friction coefficient between the columns themselves (μ_c) on old field tests to calibrate the hydraulic stability of the revetment.

For this calibration, we used 'pull-out' experiments, as described by Coeveld and Klein Breteler (2003). Pull-out tests are used to determine how well an element is clamped in a revetment. During a pull-out test, an increasing force is exerted perpendicularly on an element until it is fully lifted from the revetment. Then, the maximum force (F_u) is divided by the weight of the element (G) perpendicular to the slope ($\cos(\alpha)$). This yields a load factor (n_{fl}), which describes how well an element is clamped, see Eq. (1).

$$n_{fl} = \frac{F_u}{G \cos(\alpha)} \quad (1)$$

Over the years, numerous pull-out experiments have been conducted by Coeveld and Klein Breteler (2003), Blom et al. (2007) and Peters (2017). It has been observed that the load factor varies a lot between different experiments and types of top layer elements. The authors of these publications highlight that this variance is affected by various factors, including column type, age, temperature, and location on the slope. For in-situ locations, among the effects of many other variables, and subject to general spread, the position on the slope appears a consistent factor. Between the studies, a load factor of about 20 is a common lower bound for a pattern-placed revetment with plenty of joint filling between the columns (a well 'washed-in' revetment).

Without joint filling, the friction between the columns is solely attributed to their interaction with one another. Therefore, as a lower bound, a friction coefficient of 0.60 is used, which is a typical coefficient for concrete on concrete (Blok, 2014). For a well washed-in revetment, the joint filling will provide additional clamping thereby increasing the friction. To calibrate a friction coefficient for a well washed-in revetment, we simulated pull-out tests on different columns on the slope for varying friction coefficients between 0.60 and 0.90. The load factors from these simulations are illustrated in Fig. 3. Based on the earlier derived lower bound of the load factor for a well washed-in revetment, a friction coefficient of 0.85 is derived. For a revetment without joint filling, a friction coefficient of 0.60 is used.

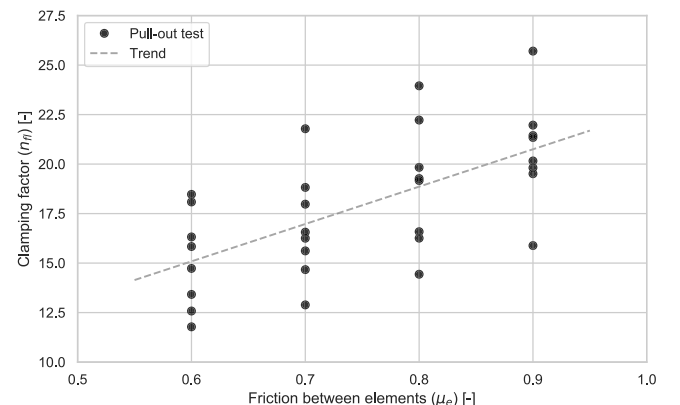


Fig. 3. Calculated load factor n_{fl} from simulated pull-out tests with the FEM model for varying friction coefficients μ_c .

2.1.3. Wave loading on a revetment

Next, we define the loading on the columns caused by wave impact. The loading can be modeled as the pressure difference caused by the wave loading on the top surface of the top layer and the pressure from the filter layer on the bottom surface of the top layer. The resulting pressure is referred to as residual pressure. In this section, we describe the wave loading and in Section 2.1.4 the filter response.

The studied top layer is composed of columns with large open joints representing 9.4% of the area and is hence permeable (Kaste and Mourik, 2016; Klein Breteler et al., 2018). As a result, the pressure in the filter layer is largely affected by the pressure caused by the wave loading. The effect of the top layer permeability is quantified by the ratio of permeabilities and the thickness of the top and filter layer, the leakage factor, as e.g. described in Klein Breteler and Bezuijen (1992) and Section 2.1.4. For a top layer composed of columns, events with large pressure gradients in space and time, such as wave impacts, likely cause damage in the form of shear and lift of the columns.

Another relevant loading could be caused by the run-down of a wave. However, because the top layer is permeable, and run-down is a relatively slow event with a moderate gradient of the head, the filter layer pressure follows the pressure above the top layer well. This is the outcome of differential equations describing based on Darcy's Law. The finding was verified by specifically instrumented scale model experiments, e.g. in Klein Breteler et al. (2012). As a result, the residual pressure is minimal; hence, within the FEM model, we only simulate the wave impact. Furthermore, due to the smooth surface of the columns, drag forces do not play a role, like in more conventional (e.g. rock) top layers.

To simulate wave impact in the FEM model, it is essential to define the wave impact location and establish a parameterization of the pressure during wave impact on the top layer for the spatial and temporal dimensions. First, we specify the wave impact location. According to Coeveld (2003a), the literature suggests that the highest waves typically impact the slope at approximately $0.5 H_s$ below the still water level (SWL). This finding was refined by Schüttrumpf (2001) based on video material for slopes of 1:4 and 1:6, indicating that the location of wave impact is lower for larger Iribarren numbers ($\xi_{m-1,0}$), as defined in Eq. (2)).

$$\xi_{m-1,0} = \frac{\tan(\alpha)}{\sqrt{s_0}} \quad \text{with} \quad s_0 = \frac{2\pi H_{m0}}{g T_{m-1,0}^2} \quad (2)$$

Where α is the slope angle of the revetment, s_0 is the wave steepness, H_{m0} is the spectral wave height, g is the gravitational constant, and $T_{m-1,0}$ the spectral wave period. We assume the significant wave height H_s equals the spectral wave height H_{m0} , and the peak wave period T_p equals about 1.1 times the spectral wave period $T_{m1,0}$ (Holthuijsen, 2007).

Peters (2017) established a relation between the location of wave run-down and wave impact. Using the horizontal and vertical particle velocity of a breaking wave, the wave impact location can be predicted in relation to the wave run-down location, denoted as z_{impact} , illustrated in Fig. 4. The equations from the study are presented in Eq. (3). When related to the still water level, the study finds that the vertical distance between the still water level and the wave impact location is approximately $0.7 H_s$.

$$\begin{aligned} \frac{z_{\text{impact}}}{H_s} &< 0.55 \xi_{m-1,0} - 0.0344 \xi_{m-1,0}^2 - 0.3 \\ \frac{z_{\text{impact}}}{H_s} &> 0.45 \xi_{m-1,0} - 0.3 \\ x_{\text{impact}} &= \frac{z_{\text{impact}}}{\tan(\alpha)} \end{aligned} \quad (3)$$

To define the wave impact location in the FEM model, we selected the model proposed by Peters (2017). This choice is based on the derivation of the equation based on physics and its validation using data from large-scale flume experiments. In contrast, Schüttrumpf

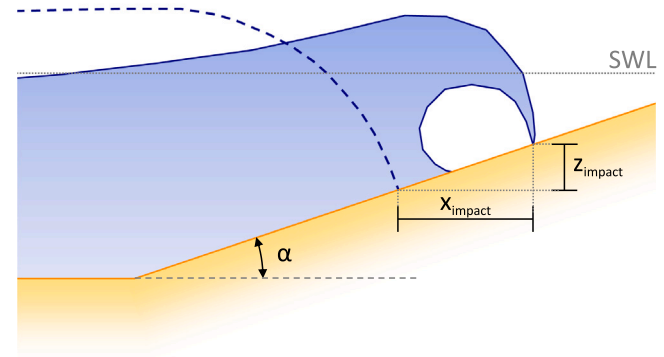


Fig. 4. Schematization of the wave impact location, relative to the run-up location: x_{impact} and z_{impact} . (blue solid line: wave impact, blue dashed line: wave run-down).

(2001) derived their equation from small-scale flume experiments. Although the rule of thumb provided by Coeveld (2003a) is simpler to implement, it significantly deviates from the other two equations, especially for higher Iribarren numbers.

Next, we focus on the pressure caused by wave impact. When a wave breaks onto the revetment, it generates a short but intense impulse. To model this impulse in the FEM model, a parameterization of the pressure is required. Since the FEM model is an explicit dynamic model, it is desirable to use a schematization defined in both spatial and temporal dimensions.

Various models in the literature describe the impulse of a breaking wave on a slope. Stive (1983) proposes a relation between the peak wave pressure, the density of the water (ρ_w), and the wave height. This relation is commonly used in combination with a triangular-shaped distributed load to model wave impact on a slope. Furthermore, Klein Breteler et al. (2012) parameterized a wave impact pressure profile in the spatial dimension using sensor data obtained from flume experiments. Peters (2017) parameterized a wave impact pressure profile in the spatial and temporal dimension using a trapezoid based on sensor data obtained from large-scale tests and a review of earlier studies. Since the parameterization by Peters (2017) is the only description considering both spatial and temporal dimensions, it is adopted in our FEM model.

$$\frac{P_{\text{peak}2\%}}{\rho_w g H_s} = 8 - 1.6 \xi_{m-1,0} - \frac{2}{(\xi_{m-1,0} - 0.2)^2} \quad (4)$$

In the spatial dimension, Peters (2017) uses the peak pressure exceeded by 2% of irregular waves ($P_{\text{peak}2\%}$), calculated using Eq. (4). Regarding the temporal dimension, the study observes that the rise time (t_r), defining the time to reach the peak pressure, is approximately 0.15 to 0.18 s and is described by Eq. (5). Following the peak pressure, the pressure gradually decreases to zero over the fall time (t_d). Peters (2017) suggests a fall time of about 3 to 4 times the rise time. In our study, we conservatively assume the fall time is 4 times the rise time to maximize the loading duration. An example of the schematization is illustrated in blue in Fig. 5. Note that the schematization does not include the wavefront, which may lead to a slight overestimation of the residual pressure between the wave impact and the wavefront.

$$t_r = 0.10 \left(\frac{P_{\text{peak}2\%}}{\rho_w g H_s} \right)^{-1} \quad (5)$$

2.1.4. Determining the filter response

With the wave loading defined, we focus on the pressure in the filter layer. The pressure in the filter layer responds to the pressure caused by the wave loading on the top layer. The extent of this response depends on the characteristics of the top layer, joint filling, and filter

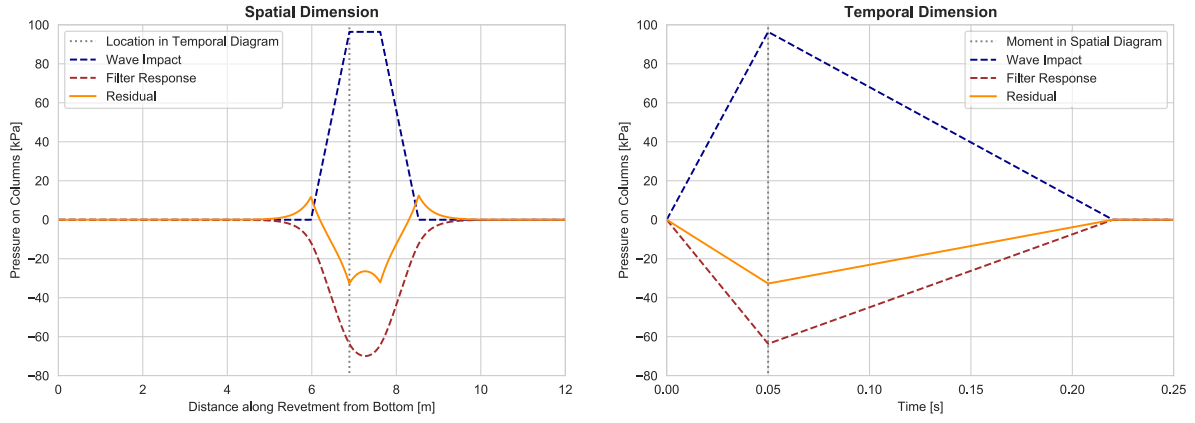


Fig. 5. Pressure evolution of wave impact and the filter response on a revetment in spatial (left) and temporal (right) dimension.

layer. To characterize this effect we use the leakage length, denoted by $\Lambda(x)$, which can be calculated using Eq. (6) (Klein Breteler et al., 2012). In this equation, the thickness of the top layer and filter layer is denoted by D and $b(x)$. The permeability of the top and filter layers are denoted by k' and k . It should be noted that we modeled the thickness of the filter layer dependent on the slope coordinate x . This modeling approach allows us to investigate the potential effect of damage caused by a deformed filter layer in subsequent analyses.

$$\Lambda(x) = \sqrt{\frac{b(x)Dk}{k'}} \quad (6)$$

Pattern-placed revetments with a top layer composed of columns have a short leakage length due to the relatively high permeability of the top layer ($\Lambda/D \approx 0.5 - 2.0$, (Peters, 2017)). Consequently, the pressure in the filter layer is highly affected by the pressure on the top surface of the top layer. The significant spatial gradients in the pressure caused by wave impact result in elevated pressures in the filter layer. As a result, the columns surrounding the wave impact location will experience a large residual pressure, which may lead to the uplift of columns.

Using the leakage length, it is possible to derive the pressure in the filter layer as a function of the pressure on the top surface of the top layer. Van der Meer et al. (2004) uses a combination of the continuity equation and Darcy's law to estimate the pressure difference between the outside and the inside of the dike. When the flow in the filter is linearized, this same principle can be applied to pattern-placed revetments, which results in Eq. (7) (Schierreck and Verhagen, 2019).

$$\Lambda(x)^2 \frac{d^2 P_F(x, t)}{dx^2} - P_F(x, t) = -P_T(x, t) \quad (7)$$

The pressure on the top surface of the top layer is denoted as $P_T(x, t)$, as given by the wave impact schematization. Solving the differential equation allows us to derive the pressure in the filter layer, denoted as $P_F(x, t)$. An example of the filter response is illustrated in red in Fig. 5.

Finally, we combine the parametrization of the wave impact pressure profile with the differential equation of the filter response. The difference between these models yields the loading profile of the residual pressure during a wave impact in both spatial and temporal dimensions, denoted as $P_R(x, t)$ and illustrated in orange in Fig. 5. In the FEM model, however, the residual pressure can only be modeled as a uniformly distributed pressure over the temporal dimension. Therefore, the loading profile of the residual pressure is averaged over the spatial dimension for each column e . This process yields an average residual pressure, denoted as $P_{R;Ave}(t)$, which is then applied as a uniformly distributed pressure to the respective column e . The entire process is illustrated in Fig. 6.

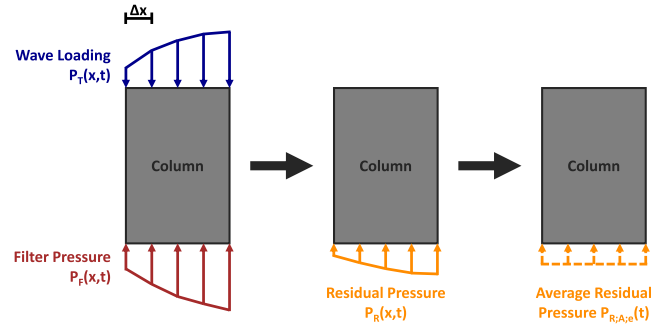


Fig. 6. Calculating the residual loading on each of the columns.

2.1.5. Defining representative loading

Next, we outline the approach for loading the pattern-placed revetment in the FEM model. In the event of a storm, a pattern-placed revetment is exposed to thousands of waves, varying in size from small to large. While simulating an entire storm in the FEM model would ideally provide the most realistic results, this would lead to undesirably long simulation times.

To identify a suitable loading scenario, we examined existing stability models (Rijkswaterstaat, 2007; Peters, 2017; Klein Breteler and Mourik, 2019). These models statically evaluate the hydraulic stability of the revetment, determining whether wave loading exceeds a critical threshold calculated based on the characteristics of the revetment. The assumption in these types of models is that the failure of the top layer of a pattern-placed revetment is more likely caused by a few high waves rather than a cumulative build-up of damage, as is common for other types of cover layers, like grass.

With the FEM model, our focus lies on dynamically evaluating the hydraulic stability. Following the methodology of earlier models mentioned, we opt to evaluate hydraulic stability based on an extreme moment during a storm rather than evaluating the entire storm. According to Holthuijsen (2007), wind waves tend to be grouped in a way that wave heights are correlated over a few waves, meaning that a high wave is typically surrounded by other higher waves. In our FEM model, we choose to model five individual waves that represent statistically the largest waves during a storm.

Then, the question arises, what is the wave height of these largest waves? One of the input parameters of our FEM model is the significant wave height (H_s). However, this parameter describes only the average height of the highest one-third of the waves and is not representative for the wave height of the largest individual waves. To address this, we chose to derive the mean wave height of the five largest subsequent waves during a storm event ($H_{\text{mean;max5}}$). In this derivation, we

assume that individual wave heights in a storm follow the Rayleigh distribution (Longuet-Higgins, 1952), as shown in Eq. (8).

$$P\left\{\bar{H} < H\right\} = 1 - \exp\left(-2\frac{H^2}{H_s^2}\right) \quad (8)$$

Using the Rayleigh distribution, we can generate random storm events for a given significant wave height. In our analysis, we use storm events with 5,000 waves, which is a typical number of waves for a storm duration of 8 to 10 h. Because the individual waves within a storm are generated based on a probability distribution, each realization of a storm differs. Multiple different storm events are generated for which the ratio between the mean wave height of the five largest subsequent waves and the significant wave height is calculated. Based on these results, a generalized extreme value distribution is fitted, as shown in Fig. 7.

In general, the mean wave height of the five largest subsequent waves is typically 1.1 to 1.4 times the significant wave height. This uncertainty is caused by the inherent randomness in the wave fields generated. Given our focus on the largest wave heights, this uncertainty results in noticeable differences for wave fields generated based on the same significant wave height. To address this uncertainty, we introduce the concept of storm intensity (i_{st}), representing the cumulative probability of the ratio between the mean wave height of the five largest subsequent waves and the significant wave height, as illustrated on the y-axis of Fig. 7. Within our FEM model, storm intensity serves as an input parameter to model this uncertainty. The wave height of the five largest subsequent waves can be calculated using the significant wave height, this wave height will be used within the FEM model to load the revetment.

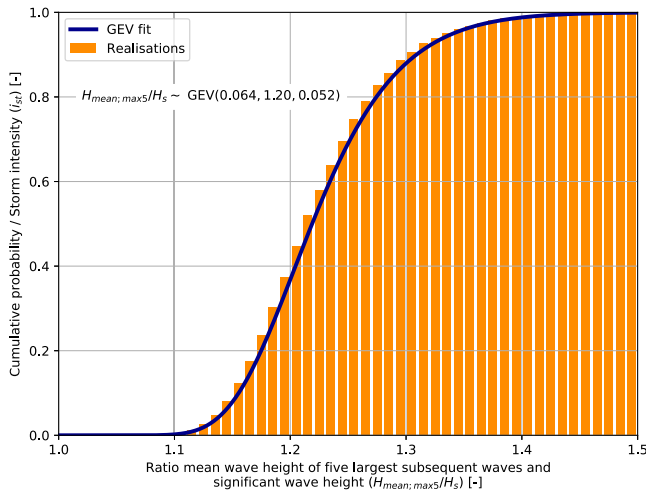


Fig. 7. Generalized extreme value distribution describing the ratio between the mean wave height of the five largest subsequent waves and the significant wave height.

The peak pressure can be calculated using Eq. (4). However, this equation can only be used to predict the peak pressure using the significant wave height. In other words, the peak pressure exceeded by 2% of the waves is predicted by the average height of the highest one-third of the waves. Ideally, we would want to know what the peak pressure of an individual wave is given the individual wave height. To correct this, first, we rewrite this equation such that the peak pressure exceeded by 2% of the waves is predicted by the average height of the highest 2% of the waves. By rewriting Eq. (8), it is determined that $H_{2\%}/H_s \approx 1.4$, leading to Eq. (9).

$$\frac{1.4 P_{\text{peak}2\%}}{\rho_w g H_{2\%}} = 8 - 1.6 \xi_{m-1,0} - \frac{2}{(\xi_{m-1,0} - 0.2)^2} \quad (9)$$

Last, we replace the statistical parameters $P_{\text{peak}2\%}$ and $H_{2\%}$ with parameters related to individual waves: the peak pressure P_{peak} and the wave height H , as shown in Eq. (10).

$$\frac{1.4 P_{\text{peak}}}{\rho_w g H} = 8 - 1.6 \xi_{m-1,0} - \frac{2}{(\xi_{m-1,0} - 0.2)^2} \quad (10)$$

It is important to note that this model is derived based on statistical wave parameters. We acknowledge that by substituting statistical parameters with non-statistical ones, we step beyond the validated application range. The predicted peak pressures may carry uncertainties. However, no other models are suitable for use within a dynamic FEM model, as discussed in Section 2.1.3. Nonetheless, the modified equation provides an order of magnitude for the peak pressure, which is sufficient for a relative analysis of the effect of damage in the subsequent sections.

In Section 3.1, we compared the hydraulic stability of a revetment as derived from the FEM model with stability models from the literature. Fig. 11, illustrates that, for the majority of data points corresponding to revetment failure, the stability models also predict failure. This emphasizes the effectiveness of our current approach, which focuses on five waves, as a fitting simplification of the loading used in the FEM model.

2.1.6. Modeling damage

As a final step, we introduce damage into the FEM model. Based on literature (Van Der Meer and Moens, 1990; Klein Breteler, 2018; Het Waterschapshuis, 2019) and analyzing the damage observed during large-scale flume experiments (Klein Breteler and Eysink, 2007; Wolters, 2016; Kaste and Mourik, 2016; Wolters and Klein Breteler, 2011; Klein Breteler and Eysink, 2005; Eysink and Klein Breteler, 2003), we selected three common types of damage for implementation: deformation, washed-out joint filling, and a missing column, as illustrated in Fig. 8. These types of damage were chosen based on their prevalence in the field and the flume experiments. To accurately represent these types of damage in the FEM model, we analyzed the data from the flume experiments, developed corresponding models for each type of damage, and implemented them into the FEM model. These models will be discussed in the subsequent paragraphs.

Deformation

When a wave breaks onto a revetment, the columns near the wave impact location are slightly lifted from the filter layer. Over time, this uplift can initiate the migration of the filter layer down the slope, causing variations in the filter layer thickness. Consequently, an S-shaped deformation of the top layer occurs, with a thinner filter layer around the wave impact zone and a thicker filter layer below it. Based on the data obtained from flume experiments, we developed a damage model for this type of deformation, named the S-profile (Van der Vegt, 2021). This damage model approximates the deformation using a sine wave of one period and is illustrated in Fig. 9. The model contains three parameters: the distance from the waterline measured from the center of the S-profile ($z_{s,\text{mid}}$), the length of the S-profile (B_s), and the amplitude of the S-profile (a_s). Additionally, we numerically implemented the effect of the deformation on the filter response in the mathematical model. This is achieved by making the filter thickness, and therefore leakage length, dependent on the location along the slope, as discussed in Section 2.1.4.

Washed-out joint filling

Caused by repeated wave loading, the granular material between the columns may wash out over time. This reduction in joint filling negatively affects clamping of the columns and therefore the hydraulic stability of the revetment. As discussed in Section 2.1.1, the effect of the joint filling on the hydraulic stability of the revetment is modeled within the friction coefficient between the columns (μ_c). Two friction coefficients were derived: one for a well washed-in revetment ($\mu_c = 0.85$) and another for a revetment without joint filling ($\mu_c = 0.60$). To


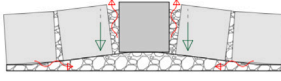
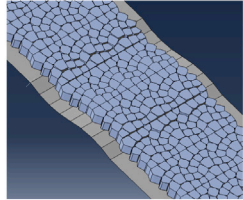

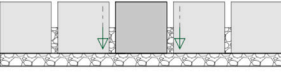
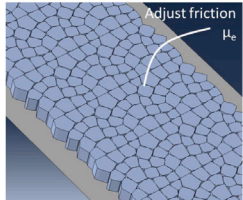

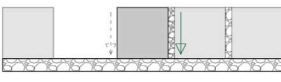
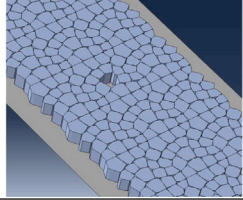
Damage	Photo	Schematisation	FEM model
Deformation caused by filter migration			
Washed-out joint filling			
Missing column			

Fig. 8. Studied types of damage in the field, schematized, and within the FEM model (photos from Kaste and Mourik (2016) and Het Waterschapshuis (2019)). Green/gray arrow: reduced clamping; Red arrow: migration of the filter and/or joint filling.

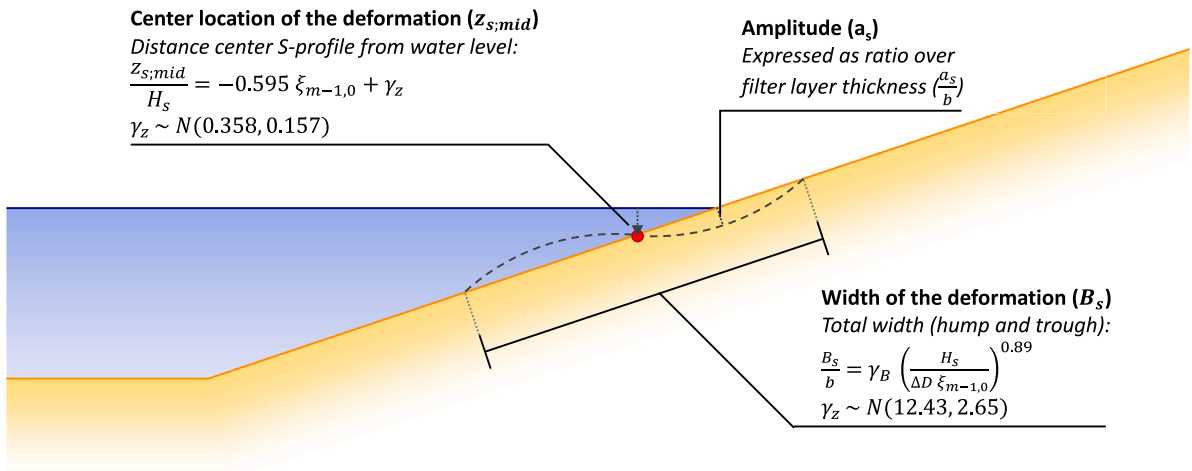


Fig. 9. Parameterization of S-shaped deformation around the wave impact zone (S-profile).

model the effect of washed-out joint filling within the FEM model, the friction coefficient between the columns is varied. The effect of this type of damage on the filter response is neglected. This simplification is expected to be conservative, as the washed-out joint filling will result in a slightly shorter leakage length.

Missing column

As outlined in Van der Vegt (2021), there are two primary reasons why a column can be missing from a revetment: third-party interference or underlying damage. The former, unrelated to the hydraulic loading, can be attributed to vandalism or the growth of woody vegetation. The latter is due to any other type of underlying damage, indicating the initiation of revetment failure. Because a missing column is simulated by removing a column from the initial geometry, the simulation resembles more closely the effects of a missing column due to third-party interference. The effect of this type of damage on the filter response is neglected. This simplification is justified, as a missing column will result in a locally shorter leakage length.

2.1.7. Model output

After simulating a FEM model, the resulting data undergoes analysis, from which several key parameters are derived which are described and presented below. These parameters aim to describe the extent of damage that has been incurred and serve as input for subsequent analysis. Damage is quantified by the uplift of a column, representing the deformation perpendicular to the slope. In instances where a column is fully lifted from the revetment, the maximum uplift is constrained to the thickness of the top layer, denoted by D . An illustrative example is depicted in Fig. 10.

- **Maximum uplift:** The maximum uplift (z_e) of all columns is a critical parameter commonly used in flume experiments. When at least one column is fully lifted, the revetment is often deemed to have failed (Kaste and Mourik, 2016). Four distinct damage categories are defined based on the maximum uplift values:

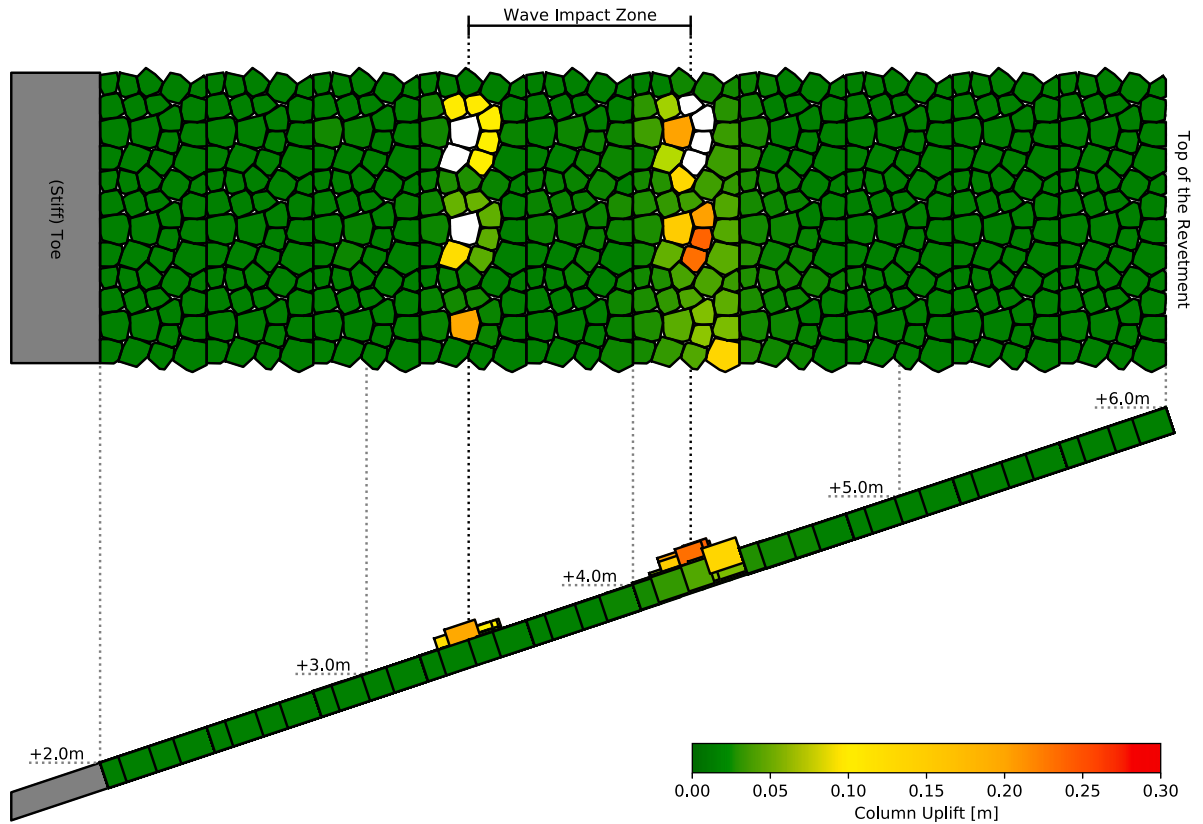


Fig. 10. Deformation of a revetment without joint filling during the peak impact of the last of five (very) extreme waves ($H_s = 2.5$ m), with colors indicating deformation relative to column thickness. A white colored column represents the column is fully lifted.

- **Damage category 1:** Little uplift of a column ($0 < z_e/D < 0.33$);
- **Damage category 2:** Significant uplift of a column ($0.33 < z_e/D < 0.67$);
- **Damage category 3:** Large uplift of a column ($0.67 < z_e/D < 1$);
- **Damage category 4:** Column came loose from revetment ($z_e/D = 1$).
- **Uplifted columns:** The number of fully lifted columns from the revetment.
- **Average final uplift:** The sum of the uplift of all columns after the last wave impact divided by the width of the model.

2.2. Surrogate modeling

Simulating five wave impacts with the FEM model can take up to three hours, making it impractical to use in the subsequent analysis. To address this, surrogate models are derived. In the following sections, we introduce the concept of surrogate models and discuss how they can be derived based on the FEM model.

2.2.1. Deriving surrogate models for (damaged) revetments

A surrogate model is a simplified approximation of the complex model, designed to emulate its behavior while avoiding the computational expenses associated with running the complex model (Kroetz et al., 2017). This approximation is derived based on the input and output from the complex model often using a machine learning algorithm or a mathematical approximation. In this study, the complex model will be the FEM model for which we aim to create four surrogate models: one for an intact revetment, and one for each type of damage discussed in 2.1.6. The objective of these models is to forecast the average final uplift (z_{final}), see Section 2.1.7. This output parameter is chosen given

its continuous nature and its ability to accurately reflect the extent of damage.

The initial step in deriving a surrogate model is to identify the relevant input parameters of the FEM model, specifically those with the most substantial effect on the hydraulic stability. Keeping the number of input parameters in the surrogate model to a minimum is crucial, as each additional parameter increases the complexity of the surrogate model, demanding a larger dataset for effective training. With over 20 distinct input parameters in the FEM model, a selection is made by assessing their effect on hydraulic stability through sensitivity analysis which is explained in Section 2.2.2. For surrogate models describing one of the types of damage, the input parameters related to this type of damage are also included.

Next, for each surrogate model, data points need to be generated to train the model. These data points are generated by running the FEM model and obtaining the average final uplift for various realizations of the input parameters of the surrogate model. These realizations are determined using a Sobol sequence. This sampling technique is chosen for its ability to provide a well-distributed and representative coverage of the parameter space (Saltelli and Ratto, 2008).

Finally, each surrogate model is trained on their respective set of data points. For the training technique, we opted to use a machine learning algorithm as it is expected that the output of the FEM model is non-linear due to the random nature of the interactions between all individual columns in the revetment. A study by Teixeira et al. (2021) shows that SVM and Kriging models are robust and perform well in terms of handling output complexity and smoothness. Another study by Bourinet (2016) found that a surrogate model using support vector regression (SVR) with SVM is capable of accurately estimating rare-event probabilities for low to moderately high dimensional problems with a smooth limit-state function. Although SVM is primarily used for classification, it can be adapted for regression tasks (SVR), making it

suitable for handling non-linearity. Based on both studies, we choose SVR to create the surrogate models. The models are made using the Python package scikit-learn (Herman and Usher, 2017).

2.2.2. Sensitivity analysis on input parameters

The FEM model comprises over 20 distinct input parameters. As discussed in Section 2.2.1, including all of these parameters in the surrogate models is impractical and unnecessary. Therefore, it is crucial to make a selection of which input parameters to include in the surrogate models based on their effect on hydraulic stability. Determining these input parameters involves two essential steps.

In the first step, a qualitative evaluation is carried out on the input parameters from the FEM model, as outlined in the Appendix. The aim is to choose five to seven parameters that have the most substantial effect on the hydraulic stability of an intact revetment. This assessment is based on relevant literature on stability models.

Subsequently, a sensitivity analysis is conducted on these identified input parameters to calculate a sensitivity index for each parameter (Saltelli and Ratto, 2008). These sensitivity indices quantify the individual contribution of each input parameter to the variability in the model output, specifically the average final uplift. A high positive sensitivity index value indicates a substantial negative effect on the hydraulic stability of the revetment. For this study, we use the 'Random Balanced Design - Fourier Amplitude Sensitivity Test' (RBD-FAST) method along with Latin Hypercube Sampling to calculate these sensitivity indices. This method proves to be a robust method suitable for limited sets of data points (Tarantola et al., 2006), making it well-applicable in our study. The set of data points necessary for the analysis is generated by running the FEM model and obtaining the average final uplift for various realizations of the previously identified input parameters. These realizations are determined using Latin Hypercube Sampling, as required by the RBD-FAST method. The sensitivity analysis is conducted using the Python package 'Sensitivity Analysis Library' (SALib) developed by Herman and Usher (2017).

2.3. Analyzing the effect of damage

Using the surrogate models, we will study the effect of the three types of damage on the hydraulic stability and failure probability.

2.3.1. Effect of damage to the hydraulic stability

The effect of damage on the hydraulic stability of the revetment is studied by comparing the difference in the stability number between damaged and intact revetments. The stability number is defined as the ratio between the loading and resistance on the revetment when the failure criterion is reached, as described in Eq. (11). In which the H_s is the significant wave height, Δ is the relative density of the top layer, and D is the thickness of the top layer. A higher stability number indicates a more stable revetment.

$$\frac{H_s}{\Delta D} \quad (11)$$

As the surrogate models forecast the average final uplift, establishing a failure criterion in terms of this parameter is key. Traditional stability models are frequently derived from flume experiments, where the assumption is that when one column is lifted from the revetment, the entire revetment is considered failed. In alignment with this, we use all FEM model results used to train the surrogate models to establish a relationship between the average number of uplifted columns per meter of the revetment and the average final uplift. This allows us to derive a failure criterion in terms of average final uplift. The stability number is then determined by analyzing the contour in the parameter space of the surrogate models where z_{final} equals the specified failure criterion.

2.3.2. Effect of damage to the failure probability

In addition to studying the effect on hydraulic stability, we also study the effect of damage on the failure probability of the revetment. The failure probability refers to the likelihood of the revetment surpassing the failure criterion within an one-year period. To investigate this, a case study is carried out on a hypothetical pattern-placed revetment on the Oostvaardersdijk. Situated along the Markermeer, a lake in the Netherlands, this dike is chosen due to the common use of the investigated type of pattern-placed revetment.

Using the surrogate models, the failure probability is calculated using a Monte Carlo simulation for various types and magnitudes of damage. To conclude, the relative effect on the failure probability is evaluated using vulnerability, see Eq. (12). Which is the ratio between the failure probability of a damaged system and an intact system subjected to identical loading conditions (Lind, 1995).

$$V = \frac{P(r_d, S)}{P(r_0, S)} \quad (12)$$

In which $P(r_d, S)$ is the failure probability of a damaged revetment and $P(r_0, S)$ the failure probability of an intact revetment. The damaged revetment is identical to the intact revetment with the only exception that any type of damage is included within the initial conditions. Practically, this means that the damage is already present before the storm event.

3. Results

In the subsequent sections, we present the results obtained in this study. Section 3.1 provides an analysis of the key parameters affecting the hydraulic stability. In Section 3.2, we present the derivation of the four surrogate models: one for an intact revetment, and one for each type of damage discussed in 2.1.6. Using these models, the effect of damage to the hydraulic stability is analyzed in Section 3.3. Lastly, Section 3.4 presents a case study examining the effect of damage to the failure probability for a hypothetical pattern-placed revetment along the Oostvaardersdijk.

3.1. Key parameters affecting hydraulic stability

This section focuses on identifying which input parameters of the FEM model have the most significant effect on the hydraulic stability of a pattern-placed revetment. All parameters are listed in the Appendix. As outlined in Section 2.2.2, this is achieved by evaluating the effect of various input parameters on the hydraulic stability through a combination of a qualitative evaluation and a sensitivity analysis using the FEM model. The input parameters with the largest effect are used within the surrogate models. Additionally, this analysis also provides insights into factors contributing to the hydraulic stability of both intact and damaged revetments, addressing the first main question of this paper.

First, we start with a qualitative evaluation by doing a literature review of the current stability models for pattern-placed revetments. Current models (Klein Breteler and Mourik, 2019), as well as calibration studies (Jongejan, 2017) and various other studies (Pilarczyk et al., 1995; Vrijling et al., 2001; Rijkswaterstaat, 2007; Peters, 2017), highlight that the hydraulic stability of a revetment is highly affected by the magnitude of the hydraulic loading. Hence, parameters such as the significant wave height and the Iribarren number are commonly used in stability models. The same studies show that in terms of resistance, the thickness and density of the top layer, and the slope of the revetment are of interest. Based on these findings, we selected six input parameters of the FEM model which we think may have the largest effect on the hydraulic stability of a revetment. An overview of these parameters is given below, along with information on the chosen lower and upper bounds for the parameter space used in the sensitivity analysis.

- **Dimensionless loading ($H_s/\Delta D$):** This parameter represents the resistance of the top layer to the hydraulic loading. It directly affects the significant wave height in the FEM model, because the top layer thickness and density are constant. The stability model of [Rijkswaterstaat \(2007\)](#) and [Peters \(2017\)](#) show that failure of the top layer is expected between a dimensionless loading of 4.0 up to 6.0. To include some margin, the dimensionless loading will be assigned a lower bound of 2.0 and an upper bound of 8.0.
- **Dimensionless leakage length (Λ/D):** The dimensionless leakage length determines how the filter responds to pressure on the top surface of the top layer. By varying this parameter, different combinations of filter layer thickness and permeability are simulated. According to [Peters \(2017\)](#), a range of 0.5 to 2.5 is typical for a top layer with columns.
- **Wave steepness (s_{0p}) and slope ($\cot \alpha$):** These parameters determine the Iribarren number and are based on the local significant wave height of the incident waves H_s and the untransformed wavelength based on the peak wave period T_p ($s_{0p} = 2\pi H_s / (g T_p^2)$). By separating wave steepness and slope the individual effect of each parameter can be evaluated. For wind waves, a typical wave steepness falls within the range of 1% to 5%. On dikes, a typical slope for a pattern-placed revetment is between 1:2.5 to 1:4.
- **Storm intensity (i_{st}):** In the FEM model, a storm is simplified into five extreme waves. The storm intensity is used to model the uncertainty between different storms as multiple storms with the same significant wave height can have a varying wave field. As defined in Section 2.1.5, the storm intensity ranges between 0.0 and 1.0.
- **Top of the revetment (z_{top}):** The top of the revetment is the distance between the water level and the top of the pattern-placed revetment. A higher top of the revetment increases the normal force within the revetment, enhancing stability. To explore the effect of this normal force, we set the top of the revetment to range between 5.5 meters and 6.5 meters above the reference level. Which is 0.5 to 1.5 meters above the still water level.

For the sensitivity analysis in this study, we use the RBD-FAST method. To perform the analysis, we generated a set containing 256 data points using Latin Hypercube Sampling and ran them with the FEM model. Uniform distributions are used for all input parameters during sampling to create a well-distributed parameter space. Each data point represents a FEM model of an intact revetment based on a different realization of the input parameters from Table 1. The output parameter used in this analysis is the average final uplift. Fig. 11 presents the results obtained from all the data points. The plots are color-coded

Table 1

Random variables with their corresponding random distributions used in the sensitivity analysis. Uniform distributions are indicated by the letter U.

Random variables	Distribution	Unit
$H_s/\Delta D$	Dimensionless loading	$U(2.0; 8.0)$
Λ/D	Dimensionless leakage length	$U(0.5; 2.5)$
s_{0p}	Wave steepness	$U(0.01; 0.05)$
i_{st}	Storm intensity	$U(0.0; 1.0)$
$\cot \alpha$	Slope	$U(2.5; 4.0)$
z_{top}	Top of the revetment	$U(5.5; 6.5)$ [REF+m]

based on the maximum uplift and the corresponding damage category, as described in Section 2.1.7.

The left pane illustrates the data points color-coded by their damage category, with the Iribarren number shown on the x-axis and the dimensionless loading on the y-axis. Two stability models, namely ‘VTV2004’ ([Rijkswaterstaat, 2007](#)) and the model proposed by [Peters \(2017\)](#), are also featured in the figure. The VTV2004 stability model provides two curves: the upper curve signifies a high likelihood of failure, denoted as ‘Unsafe,’ while the lower curve indicates a low likelihood of failure, marked as ‘Safe.’ The region between these curves is labeled as ‘Unknown,’ signifying uncertainty where failure may occur depending on the state of the pattern-placed revetment. The stability model by [Peters \(2017\)](#) is derived based on when the first column is fully lifted from the revetment. Therefore, this curve should predict at which dimensionless loading a column is fully lifted from the revetment (damage category 4). In the figure, it can be seen that the lower bound of the data points with damage category 4 are relatively close to both stability relations. This gives confidence in the proper calibration of the FEM model for intact revetments and the applied simplification in defining the representative loading using the five largest subsequent waves, highlighting the reliability of the results.

The right pane depicts a similar graph with the dimensionless leakage length plotted on the x-axis. From this figure, it becomes clear that the dimensionless leakage length has a significant effect on the hydraulic stability of a revetment. This can be attributed to the fact that for top layers composed of columns, a longer leakage length makes it more difficult for the filter pressure to dissipate. This results in an increased residual pressure on the columns, thereby causing the revetment to fail at a lower dimensionless loading.

Next, a sensitivity analysis using the RBD-FAST method is conducted on the set of data points, yielding the results depicted in Fig. 12. For each of the input parameters, the first-order sensitivity index S_1 is calculated along with its corresponding 95% confidence interval. The sensitivity index measures the individual contribution of each input

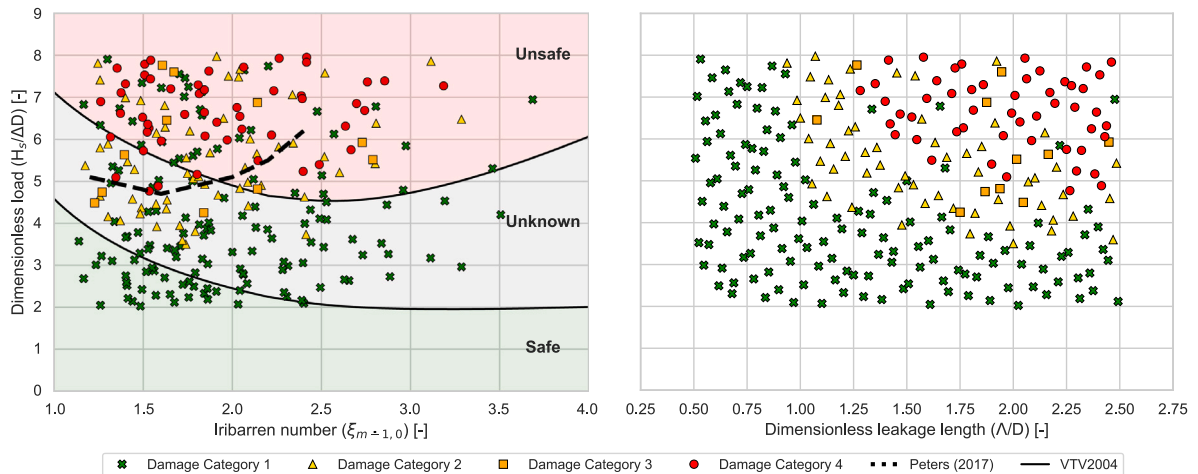


Fig. 11. Maximum uplift for each data point with the stability model from VTV2004 ([Rijkswaterstaat, 2007](#)) and [Peters \(2017\)](#).

parameter to the model output's variability, which is the average final uplift. A high positive S_1 value suggests a substantial negative effect on the hydraulic stability of the revetment.

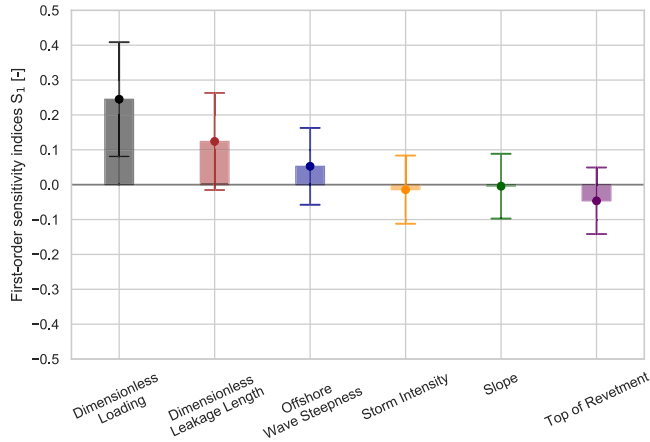


Fig. 12. First-order sensitivity indices representing the effect of parameters on the hydraulic stability of an intact revetment, along with the corresponding 95% confidence intervals.

Fig. 12 indicates that the hydraulic stability is primarily negatively affected by an increase of the dimensionless loading or dimensionless leakage length, which can also be seen in the right pane of Fig. 11. Given that the top layer thickness and density are constant, it can be concluded that the significant wave height and leakage length have the largest effect. Additionally, an increase in wave steepness also negatively affects the hydraulic stability as it increases the loading on the slope for a plunging breaker, see also Eq. (10). Furthermore, the results also show that lowering the top of the revetment negatively affects the hydraulic stability. This is consistent with Vrijling et al. (2001) and Peters (2017) who suggest that, as a higher top of the revetment implies a larger length, the normal force of the revetment around the water line increases. This improves the clamping of the columns and, therefore, the hydraulic stability of the revetment.

Minimizing the number of input variables in the surrogate models is crucial to keep the required dataset for training the surrogate model small enough. Therefore, we aim to select a maximum of three input parameters, excluding those describing damage. We opted to include the dimensionless loading and the dimensionless leakage length, as both substantially affect the hydraulic stability. Additionally, we chose to include wave steepness, given that its effect on hydraulic stability and the corresponding confidence interval are slightly larger than those of the top of the revetment.

3.2. Predicting damage with a surrogate model

Next, the surrogate models are derived, comprising one for an intact revetment and one for each type of damage (deformation, loss of joint filling, and a missing column). The initial step involves generating four sets of data points to train each surrogate model. Based on the previous section, the dimensionless loading, dimensionless leakage length, and wave steepness are used as input parameters. During sampling, we use the uniform distributions also used in the sensitivity analysis. Additionally, for the surrogate models for each type of damage, the respective parameters related to describing that type of damage are also included, which are described below.

- **Uncertainty of the location of the S-profile (γ_s):** The uncertainty about the (center) location of the deformation is modeled by a normal distribution, as outlined in Van der Vegt (2021).

- **Uncertainty of the width of the S-profile (γ_B):** The uncertainty about the width of the deformation is modeled by a normal distribution, as outlined in Van der Vegt (2021).
- **Ratio of amplitude S-profile over filter layer thickness (a_s/b):** The greater the ratio, the more significant the deformation. Given the assumption in the S-profile model that deformation is exclusively due to filter migration, it cannot exceed the filter layer thickness. Consequently, this parameter is represented by a lower bound of 0.0 and an upper bound of 1.0.
- **Friction coefficient between columns (μ_c):** Since joint filling is not physically modeled, the additional clamping/resistance it imparts is calibrated through the friction between columns. In Section 2.1.2, a friction coefficient of $\mu_c = 0.85$ for a well-washed-in revetment and $\mu_c = 0.60$ for a revetment without joint filling is derived. Therefore, a range between 0.60 to 0.85 is used for this parameter.
- **Location of the missing column below the still water level (SWL) (z_c):** Represents the depth, in meters, below the SWL at which a column is removed from the revetment. Given that the wave impact location is below SWL, the upper bound is set at 0.0 meters (at SWL). The lower bound is defined slightly above the bottom of the revetment at 2.5 meters below SWL.
- **Offset of the missing column from the center line of the revetment (x_c):** Introduces variability to avoid consistently removing the same column at the same depth z_c . It is defined within a range of -1.3 m to 1.3 m from the centerline of the revetment. Given that the total width of the model is 3.27 m, this maximum offset of 1.3 meters ensures that columns near the boundary of the revetment (those with boundary conditions) are not removed.

The surrogate models will predict the average final uplift. To achieve this, each surrogate model needs to be trained on a set of data points, containing different realizations of the input parameters and the corresponding average final uplift calculated using the FEM model. For each surrogate model we generated a unique set of data points. A comprehensive summary of all input parameters and their random distributions used is provided in Table 2. To ensure the surrogate models predict well over the whole parameter space, the data points must be well-distributed in the parameter space. This is achieved by using a uniform distribution for most parameters and using a Sobol sequence as a sampling technique to generate the data points.

Before delving into the training of the surrogate models, it is necessary to establish a failure criterion. Given that surrogate models provide forecasts for the average final uplift, determining a critical value for failure proves challenging due to the abstract nature of this parameter. Using the four sets of data points for the surrogate models, we related the average final uplift to the number of fully lifted columns per meter width of the revetment, as illustrated in Fig. 13.

Using the relationship depicted in Fig. 13 a practical failure criterion for the average final uplift in terms of fully lifted columns per meter width of the revetment can be established. Currently, the most prevalent failure criterion in other models is to deem a pattern-placed revetment as 'failed' if at least one column is fully lifted from the revetment. Translated into the metric of fully lifted columns per meter, this means disallowing any fully lifted columns, resulting in zero occurrences per meter. Referring to Fig. 13, this would correspond to an average final deformation z_{final} of approximately 0.15 as the failure criterion.

Finally, the four surrogate models are trained on their respective sets of data points. For the training technique, we use the SVR machine learning algorithm outlined in Section 2.2. Each surrogate model is then calibrated by fine-tuning the hyperparameters, which are parameters that control the machine learning algorithm and are set before the learning process begins. The values for these parameters are not learned from the data but are determined by the user and affect the behavior and performance of the model. Since our focus is on evaluating the

Table 2

Used probability distributions within the different sets of data points. Uniform distributions are indicated by the letter *U*, normal distributions are indicated by the letter *N*.

Random variables	Distribution	Unit
Input parameters applicable to all surrogate models		
$H_s/\Delta D$	Dimensionless loading	$U(2.0; 8.0)$
A/D	Dimensionless leakage length	$U(0.5; 2.5)$
s_{0p}	Wave steepness based on untransformed wave length	$U(0.01; 0.05)$
Surrogate model 1: No Damage (128 data points)		
No additional input parameters are required		
Surrogate model 2: Deformation S-Profile (224 data points)		
γ_z	Uncertainty of the location of S-Profile (see Fig. 9)	$N(0.358; 0.157)$
γ_B	Uncertainty of the width of S-Profile (see Fig. 9)	$N(12.43; 2.65)$
a_s/b	Ratio of amplitude S-profile over filter layer thickness	$U(0.0; 1.0)$
Surrogate model 3: Reduced Clamping (160 data points)		
μ_c	Friction coefficient between columns	$U(0.60; 0.85)$
Surrogate model 4: Missing Column (192 data points)		
z_c	Location of the missing column below the still water level	$U(0.0; -2.5)$
x_c	Offset of the missing column from the center line of the revetment	$U(-1.3; 1.3)$

relative effect of damage the hydraulic stability, we calibrate the hyperparameters until the results of the surrogate model for an intact revetment match those obtained from the stability model developed by Peters (2017).

For deformed revetments and revetments with washed-out joint filling, the intact scenario is included in the parameter space. This is achieved by setting the input parameter related to the amplitude over filter layer thickness ratio (a_s/b) to 0 for the surrogate model representing deformation and the friction between columns (μ_c) to 0.85 for the surrogate model representing reduced clamping. This facilitates the calibration of these models to match the model of Peters. However, for the surrogate model representing a revetment with a missing column, the intact scenario is not present within its parameter space, as all data points involve one column being removed from the revetment. Given the largely consistent calibrated hyperparameters between the other three models, we opted to calibrate the surrogate model for a missing column using the hyperparameters derived from the surrogate model representing the intact revetment.

After calibration, we found that the calibrated hyperparameters of the models are largely consistent between the models. This gives us confidence that neither of the models is overfitting or underfitting. Panel (a) of Fig. 14 displays the stability curves for all four models. Because the slope is not an input parameter in the surrogate models, the parameter space from the Iribarren number reaches between 1.50 and

3.33. Note that in the sensitivity analysis in Section 3.1, the slope was also sampled, resulting in a parameter space of the Iribarren number between 1.12 and 4.00. For larger Iribarren numbers, we observed larger differences between the stability curves. This may be attributed to the varying density of data points at higher Iribarren numbers. Specifically, as the Iribarren number is dependent on the square root of the wave steepness, the density of data points for lower Iribarren numbers is higher than for larger Iribarren numbers.

3.3. Effect of damage on the hydraulic stability

The effect of damage to the hydraulic stability is investigated by using the surrogate models to derive stability curves. A stability curve illustrates the relationship between the stability number and the Iribarren number. It proves a representation of the hydraulic stability under varying conditions and can be used to identify the critical dimensionless loading where the hydraulic stability of the revetment may be compromised. The stability number is determined by analyzing the contour in the parameter space of the surrogate models where z_{final} equals the specified failure criterion of 0.15. For each type of damage, stability curves for various magnitudes of damage are derived, as illustrated in Panes (b), (c), and (d) of Fig. 14. The stability curve representing an intact revetment is obtained using its respective surrogate model, while

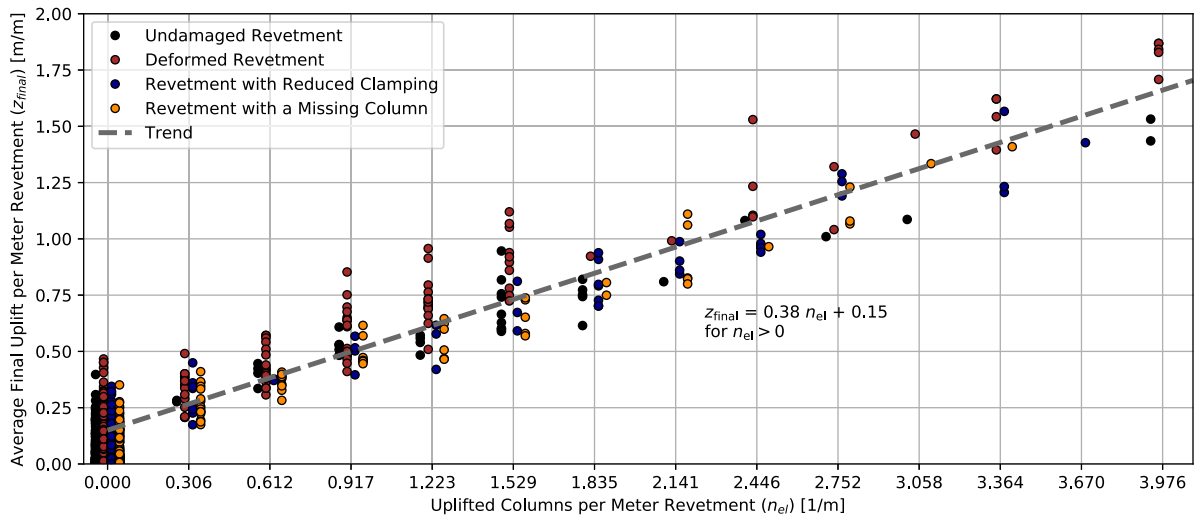


Fig. 13. The average final uplift in relation to the number of columns fully lifted from the revetment.

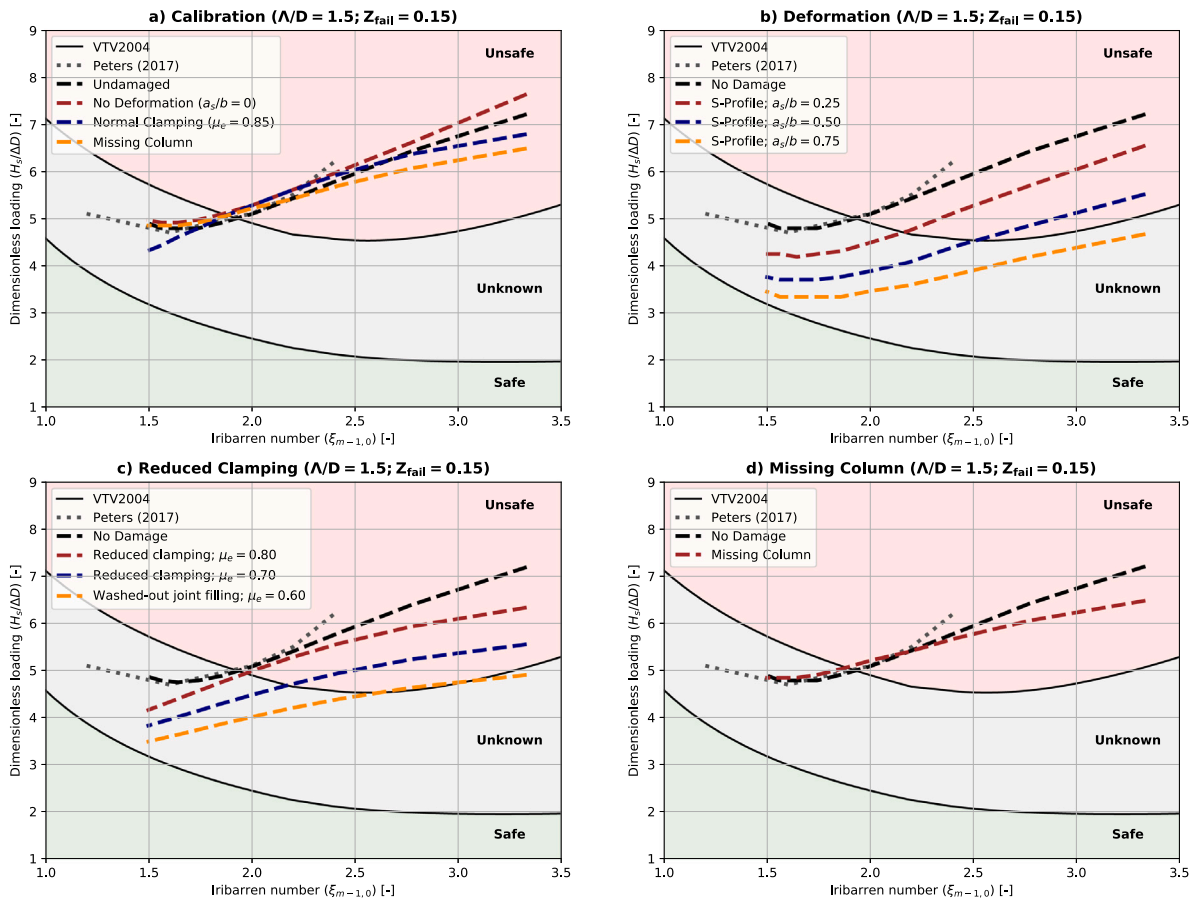


Fig. 14. Stability curves obtained from the surrogate models after calibration in Pane (a), and the different types of damage in Pane (b), (c), and (d).

the other curves are derived using the surrogate model specific to each type of damage.

In Pane (b) of Fig. 14, stability curves are shown for a deformed revetment. It is observed that, for a deformed revetment, the stability curves follow a similar shape to that of an intact revetment. However, the model clearly shows that the stability number decreases as the amplitude of deformation increases. This decrease can be primarily attributed to two aspects. First, the columns on the 'hump' of the deformation experience reduced clamping due to the concave curvature of the deformation. Additionally, due to the deformation, the filter layer thickness varies, resulting in a thicker filter layer under the hump of the deformation and a thinner filter layer below the trough. An increase in filter layer thickness leads to higher filter pressure, thereby increasing the residual pressure on the columns. Generally, due to deformation, columns on the hump of an S-profile have lower hydraulic stability and are more prone to be fully lifted from the revetment. The (negative) effect of both aspects depends on the amplitude of the deformation; a larger amplitude will lead to lower hydraulic stability.

In Pane (c) of Fig. 14, the effect of washed-out joint filling on hydraulic stability is illustrated. Overall, the reduction in hydraulic stability is less significant than that of deformation. Nonetheless, the results suggest that washed-out joint filling can still lead to a 25% decrease in the stability number. This reduction in hydraulic stability can be attributed mainly to a decrease in clamping, making the columns more prone to being lifted from the revetment by the filter pressure.

In Pane (d) of Fig. 14, the effect of a missing column on the hydraulic stability is shown. The results indicate minimal differences in the stability number compared to an intact revetment for lower Iribarren numbers. According to the literature, these mild consequences are expected. Coeveld et al. (2005), Klein Breteler and Eysink (2007)

conducted flume experiments on an initially damaged Basalton revetment to study the progression of damage. Before the experiment, three columns were removed in three different places. After several experiments, including one with two missing columns, no additional columns were fully lifted from the revetment, and only some locally washed-out joint filling and migrated filter material were observed. The difference between both stability lines increases for larger Iribarren numbers. However, as discussed in the previous section, this may be attributed to a lower density of data points for larger Iribarren numbers.

3.4. Effect of damage on the failure probability

Lastly, we study the effect of damage on the failure probability of a revetment. This is achieved by calculating the failure probability for various types and intensities of damage using the surrogate models. As we are mainly interested in the relative effect of damage on the failure probability, we quantify this using vulnerability, as defined in Section 2.3.2 and described by Lind (1995).

The failure probabilities are calculated for a fictional pattern-placed revetment on the Oostvaardersdijk, which is situated along the Markermeer (a lake in the Netherlands). This dike is chosen due to the common use of the investigated type of pattern-placed revetment. The cross-section in Fig. 15 illustrates the pattern-placed revetment under consideration. Its dimensionless leakage length is calculated to be 1.28, with the bottom of the revetment at NAP+0.50 m and the top at NAP+6.0 m.

The water depth at the toe of the dike is 5 m. The significant wave height is modeled stochastically, and its random distribution is derived from statistics used in Dutch guidelines for dike assessment (Rijkswaterstaat, 2017). Specifically, the distribution is derived for location

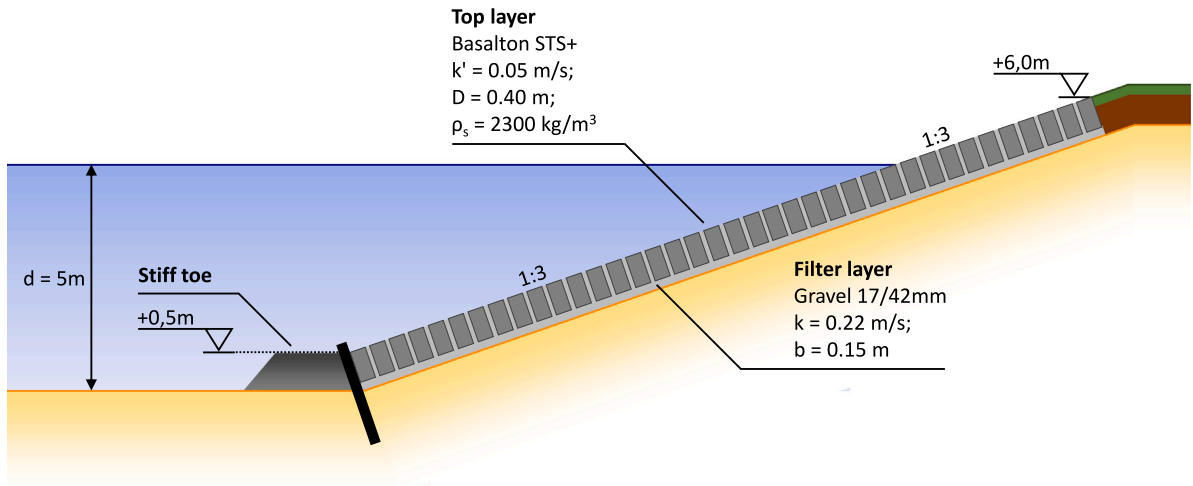


Fig. 15. Cross-section of the analyzed pattern-placed revetment.

'MM_2.82.dk_00189' using the WBI2017 databases and the software Hydra-NL (Duits, 2020). Additionally, the random distribution for wave steepness is assumed to be a normal distribution with a mean of 0.03 and a coefficient of variance of 10% (Caires and van Gent, 2010).

Subsequently, using the surrogate models, a Monte Carlo simulation is conducted to estimate the failure probability for various types and magnitudes of damage. The outcomes of these simulations are depicted in Fig. 16. Based on these results, the vulnerabilities are calculated and presented in Table 3.

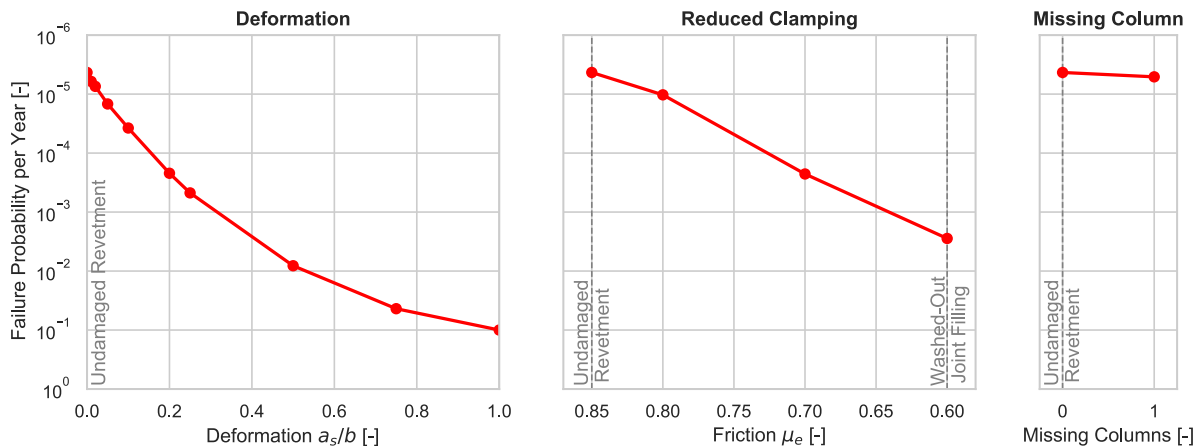
Table 3
Failure probability and vulnerability for different types of damage ($n = 10^7$ samples).

Deformation (S-profile)	Parameter	Failure probability	Vulnerability
No Damage	$a_s/b = 0.00$	$4.00 \cdot 10^{-6}$	1
Very Small S-profile	$a_s/b = 0.10$	$3.80 \cdot 10^{-5}$	10
Small S-profile	$a_s/b = 0.25$	$4.73 \cdot 10^{-4}$	100
Medium S-profile	$a_s/b = 0.50$	$8.14 \cdot 10^{-3}$	2,000
Large S-profile	$a_s/b = 0.75$	$4.28 \cdot 10^{-2}$	10,000
Reduced clamping	Friction	Failure probability	Vulnerability
No Damage	$\mu_c = 0.85$	$4.00 \cdot 10^{-6}$	1
Small Reduction Clamping	$\mu_c = 0.80$	$1.00 \cdot 10^{-5}$	3
Large Reduction Clamping	$\mu_c = 0.70$	$2.26 \cdot 10^{-4}$	50
No Joint Filling	$\mu_c = 0.60$	$2.80 \cdot 10^{-3}$	700
Missing column	Columns	Failure probability	Vulnerability
No Damage	0	$4.00 \cdot 10^{-6}$	1
Missing Column	1	$5.00 \cdot 10^{-6}$	1.25

The results are consistent with the findings of our analysis on the effect of damage on the hydraulic stability. From this analysis, we can conclude that among the studied types of damage, deformation has the largest effect on the failure probability, with a vulnerability of up to 2,000 for a medium-sized S-profile. It is important to note that even a small S-profile can have a significant effect. Furthermore, washed-out joint filling can also have a relatively large effect on the failure probability, with a vulnerability of up to 700. Finally, a missing column has a relatively small effect on the failure probability with a vulnerability of 1.25, which is consistent with the findings of the stability analysis and the experiments conducted by Coeveld et al. (2005), Klein Breteler and Eysink (2007).

4. Discussion

This paper introduces a methodology to investigate the hydraulic stability of (initially) damaged pattern-placed revetments using Finite Element Modeling (FEM). The study focuses on analyzing the behavior of top layers composed of columns, using Basalton STS+ as an example. A literature review was conducted to analyze various types of damage observed in flume experiments, including those with Basalton or basalt columns (Van der Vegt, 2021). The results reveal similarities in types of damage, suggesting the potential applicability of the methodology to different types of top layers, such as basalt, C-Star®, and Hydroblocks®. However, further substantiation of this hypothesis could be achieved by applying the methodology presented in this paper to other types of top layers.

Fig. 16. Failure probability for different types and magnitudes of damage ($n = 10^7$ samples).

To reduce simulation time in our FEM model, we simplified the hydraulic loading by condensing a storm event, typically comprised of thousands of waves, into five extreme waves. This simplification implies almost instantaneous revetment failure by surpassing a critical loading, without accounting for the cumulative buildup of damage over time. In reality, the hydraulic stability of the top layer is predominantly affected by the time-dependent behavior of other parts of the revetment, such as by the load-history of wave loading (Vrijling et al., 2001; Peters, 2017), filter layer (e.g. deformation caused by filter migration) and joint filling (Van der Vegt, 2021). Currently, the only model capable of simulating time-dependent behavior is an older numerical model known as 'Zsteen' (Hofland and Klein Breteler, 2005). This model uses simplified physics and the Forchheimer equation to simulate the pressure in the filter layer over time. However, no studies have been done on the effect of damage on the hydraulic stability using this model. Further research could concentrate on exploring the time-dependent behavior of the filter layer, joint filling, and the development of various types of damage to create a time-dependent stability model for (damaged) revetments.

Our study relies on FEM, which, while effective, introduces constraints in modeling. This becomes apparent as physically modeling the joint filling will cause the simulation time to increase by a thirty-fold (up to 90 h). To address this, we calibrated the friction coefficient between top layer columns to approximate the additional resistance from joint filling. However, this practical workaround has limitations, as the absence of a physical model for joint filling may introduce uncertainties in simulation outcomes. Therefore, findings should be interpreted, recognizing that the representation of the joint filling may be limited in the current model. Future research could explore alternative modeling techniques or validation methods to enhance the accuracy of simulating the effect of joint filling within the FEM model.

Conducting numerous simulations with the FEM model poses a challenge due to the relatively long simulation time. Surrogate modeling provides a practical solution to these computational challenges and complexities, though it comes with certain limitations. Surrogate models provide a good approximation within the bounds of the sampled space of the key input parameters but should be handled carefully outside these bounds as not all physical behavior might be represented properly. The balance between including an optimal number of input parameters and maintaining computational efficiency may lead to oversimplification, potentially neglecting factors affecting hydraulic stability. To address this, we first performed a sensitivity analysis to identify the key parameters, which were subsequently used to create the surrogate models.

Validating the surrogate models in this study poses a challenge. While the FEM model is validated against stability models, as depicted in Fig. 11, the validation of surrogate models proves to be more challenging due to the absence of models and data from physical experiments on damaged revetments. For each studied type of damage, a separate surrogate model is trained. While this approach allows us to examine isolated cases of various types of damage, in reality, different types of damage often occur simultaneously. Flume experiments also show that when a pattern-placed revetment fails, multiple types of damage have occurred (Klein Breteler and Eysink, 2007; Wolters, 2016; Kaste and Mourik, 2016; Wolters and Klein Breteler, 2011; Klein Breteler and Eysink, 2005; Eysink and Klein Breteler, 2003). This makes it extremely challenging to use data from physical experiments to validate the surrogate models. A combination of different types of damage will always lead to a lower hydraulic stability than when these types of damage are assessed as isolated cases. This interaction is complex and out-of-scope in this study. Nevertheless, it is especially relevant for dike managers to know what the consequences are of different combinations of damage, and what the most critical combinations are. Future research could extend the FEM model to examine the interaction between different types of damage.

Deformation around the wave impact zone is shown to substantially affect the hydraulic stability of the top layer. In our FEM model, we assumed that deformation is exclusively induced by filter migration. Therefore, we implemented a varying filter layer thickness based on the shape of the deformation. However, it is crucial to note that this assumption might be conservative if other factors, such as consolidation, creep, or liquefaction, contribute to or cause the deformation. Previous work by Klerk et al. (2021) examined the Probability of Detection (PoD) for different types of damage to revetments. While no specific PoD was determined for a deformed pattern-placed revetment, a PoD of 0.3 was derived for a deformed grass slope. This shows that detecting deformed revetments by eye is challenging due to small elevation differences over a long slope. In addition, detecting damage is even more difficult for pattern-placed revetments due to their numerous separate elements (Klerk et al., 2021). Nevertheless, the effect of deformation on the hydraulic stability of pattern-placed revetments is significant. Alternative surveying methods, such as drone-mounted LIDAR measurements, may be necessary to enhance accuracy and detection capabilities during inspections.

Washed-out joint filling is simulated in the FEM model by adjusting the friction coefficient between columns (μ_c) from 0.85 to 0.60 (see Sections 2.1.2 and 2.1.6). Klein Breteler (2018) describes that columns with minimal joint filling can still be tightly clamped. This may be because only a small amount of joint filling is required to effectively transfer normal force between columns. This implies that, for example, when half of the joint filling is washed-out, the friction coefficient is still relative high (μ_c near 0.85). It is only when this last bit of joint filling is washed out that the additional resistance provided by the joint filling dissipates, reducing μ_c to 0.60. These findings, combined with the results of the study, suggest that washed-out joint filling primarily affects the hydraulic stability of the top layer when nearly all joint filling is washed out.

Within the FEM model, we studied the effect of a missing column by removing it from the initial geometry. However, this approach may not always be accurate for every scenario. There are two primary reasons why a column can be missing from a revetment: third-party interference or underlying damage. Instances of third-party interference, such as vandalism, often result in minimal damage beyond the absence of the column. However, when underlying (structural) damage is the cause of a missing column, this can signal the initiation of revetment failure and, therefore, require immediate maintenance efforts (Van der Vegt, 2021). The way we modeled a missing element in the FEM model more closely represents the scenario where a column is absent due to third-party interference. Given the significant differences between these two causes, it is crucial to differentiate between them during inspections and to report not only the occurrence of a missing column but also to try to identify the underlying cause.

5. Conclusion and recommendations

This study presents an approach and model for estimating the effect of assumed initial damage to the hydraulic stability of a pattern-placed revetment on a dike using finite element modeling (FEM). The output from the FEM model was successfully validated with existing stability relations for intact pattern-placed revetments. This demonstrates the potential of finite element modeling as an alternative to physical experiments.

Because a FEM model is impractical to use within analyses, we created four surrogate models: one for an intact revetment and one for each type of damage (deformation, loss of joint filling, and a missing column). While deriving the models, we found that the dimensionless loading, dimensionless leakage length, wave steepness, and the top of the revetment have the largest impact on the hydraulic stability of the revetment.

Using the surrogate models, we studied the effect of different types and magnitudes of damage on the hydraulic stability and failure probability, a summary of these results is shown in Table 4. The results show

that deformation caused by filter migration around the wave impact zone has the largest effect on the hydraulic stability of a revetment, followed by washed-out joint filling. A missing column typically has a limited immediate effect when it is there is no other (structural) damage.

Table 4

Quantification of the effect of damage to the hydraulic stability and failure probability of pattern-placed revetments subjected to wave loading.

Damage	Decrease of stability number	Vulnerability case study
Small S-profile ($a_s/b = 0.25$)	14%	100
Medium S-profile ($a_s/b = 0.50$)	23%	2,000
Large S-profile ($a_s/b = 0.75$)	30%	10,000
Washed-out Joint Filling ($\mu_e = 0.60$)	29%	700
Missing Column (No. = 1)	0% - 1%	1

Insights obtained from this study can be used to prioritize maintenance efforts in risk-based maintenance of pattern-placed revetments. The presented approach can be extended with additional types of damage such as deformed toe structures and growth of woody vegetation, and towards other types of top layer elements such as basalt, C-Star, and Hydroblocks. Finite element modeling appears suitable for estimating the effect of damage, which can then be used to set up targeted flume experiments to formulate and validate assessment rules for damaged pattern-placed revetments.

Further research could concentrate on the time-dependent behavior of pattern-placed revetments, and the progression of different types of damage over time. This could ultimately lead to a time-dependent stability model to evaluate the hydraulic stability of (damaged) pattern-placed revetments. This study only assessed isolated cases of damage. In reality, different types of damage occur simultaneously and will always lead to a lower hydraulic stability than when these types of damage are assessed as isolated cases. This is especially relevant for dike managers to know what the consequences are of different combinations of damage, and what the most critical combinations are. Future research could extend the FEM model to study the interaction between different types of damage.

CRedit authorship contribution statement

N. van der Vegt: Writing – original draft, Visualization, Software, Methodology, Formal analysis, Conceptualization, Data curation, Investigation, Supervision. **W.J. Klerk:** Writing – review & editing, Supervision, Funding acquisition, Conceptualization, Methodology. **D.J. Peters:** Writing – review & editing, Supervision, Conceptualization, Methodology. **M.R.A. van Gent:** Writing – review & editing, Supervision, Conceptualization, Methodology. **B. Hofland:** Writing – review & editing, Supervision, Conceptualization, Methodology.

Declaration of competing interest

The authors declare that they have no known competing financial interests or personal relationships that could have appeared to influence the work reported in this paper.

Data availability

The source of the data is explained in the article. The FEM model is available on GitHub: https://github.com/nielsvandervegt/fem_patte_rnplacedrevetment..

Acknowledgments

This work was (partly) financed by NWO Domain Applied and Engineering Sciences through the research programme All-Risk with project number P15-21.

Appendix. Parameters

Table 5 provides an overview of all parameters defined in the FEM model, along with their respective default values. In the analysis conducted for this study, if a parameter is not explicitly defined, the default value is used.

Table 5

Parameters defined in the FEM model with their respective default values.

Symbol	Description	Value	Units
Geometry			
B_m	Width of the model	3.00	[sets]
$\cot \alpha$	Slope	3.00	[–]
d	Water depth	5.00	[m]
z_{top}	Top of the revetment	6.0	[REF+m]
z_{bot}	Bottom of the revetment	2.0	[REF+m]
g	Gravitational acceleration	9.81	[m/s ²]
Wave Loading			
H_s	Significant wave height	<i>Varies</i>	[m]
T_p	Peak period	<i>Varies</i>	[s]
i_{st}	Storm Intensity	0.50	[–]
s_{0p}	Wave steepness ($s_{0p} = 2\pi H_s / (g T_p^2)$)	<i>Varies</i>	[–]
ρ_w	Density of the water	1025	[kg/m ³]
Top Layer			
D	Thickness of the top layer	0.30	[m]
Λ	Leakage length	<i>Varies</i>	[m]
ρ_c	Mass density of the columns (without joints)	2240	[kg/m ³]
E_c	Young's modulus of the columns	50.0	[GPa]
ν_c	Poisson's ratio	0.20	[–]
μ_e	Friction between columns (with joint filling)	0.85	[–]
μ_f	Friction between columns and the filter layer	0.60	[–]
Numerical			
dx	Step in space for determining loading	0.01	[m]
dt	Step in time for determining loading	0.01	[s]

References

- Bezuijen, A., 1984. In-situ meting van de lekengte in een taludbekleding van gezette steen (Dutch) [In-situ measurement of leakage length in pattern-placed revetments]. Technical Report CO-269630, Laboratorium voor grondmechanica Delft, Delft, URL <http://resolver.tudelft.nl/uuid:14cadf51-71dc-4c3e-9c0a-eea3caf440f3>.
- Bezuijen, A., Wouters, J., Den Adel, H., 1990. Numerical simulation of the motion of a loose revetment block. Coastal Eng. Proc. 1 (22), <http://dx.doi.org/10.1061/9780872627765.122>.
- Blok, R., 2014. Tabellen Voor Bouwkunde En Waterbouwkunde (Dutch) [Tables for Civil and Hydraulic Engineering.]. ThiemeMeulenhoff b.v., ISBN: 9789006900453.
- Blom, J.A.H., Peters, D.J., 't Hart, R., van Casteren, A.J.E.J., Vrijling, J.K., 2007. Field tests on clamping in block revetments. In: Coastal Structures 2007. pp. 526–537. http://dx.doi.org/10.1142/9789814282024_0047.
- Bourinet, J.M., 2016. Rare-event probability estimation with adaptive support vector regression surrogates. Reliab. Eng. Syst. Saf. 150, 210–221. <http://dx.doi.org/10.1016/j.res.2016.01.023>.
- Burger, A.M., 1983. Taludbekleding van gezette steen, grootschalig gidsonderzoek (Dutch) [Pattern-placed revetments, large-scale experiments]. Technical Report M1795 / M1881, Waterloopkundig laboratorium en laboratorium voor grondmechanica, Delft, URL <http://resolver.tudelft.nl/uuid:df1a6c70-0d5d-4bfa-a5f8-47970b989964>.
- Caires, S., van Gent, M.R.A., 2010. Wave height distribution in constant and finite depths. In: Coastal Engineering Proceedings. 1, <http://dx.doi.org/10.9753/icce.v33.waves.15>.
- Coeveld, E.M., 2003a. Invloed van golfklappen op stabiliteit: literatuurstudie (Dutch) [The influence of wave impacts on stability: a literature review]. Technical Report H4134, WL | Delft Hydraulics, Delft, URL <http://resolver.tudelft.nl/uuid:9be542d5-1655-45e3-85cc-78e3c0278d13>.

- Coeveld, E.M., 2003b. Software-ontwikkeling en toepassing voor kwantificering van golfklappen (Dutch) [Software development and application for quantification of wave impacts]. Technical Report H4238, WL | Delft Hydraulics, Delft, URL <http://resolver.tudelft.nl/uuid:507d7dc9-a544-44b5-bb84-22d26daa45a2>.
- Coeveld, E., Klein Breteler, M., 2003. Invloed klemming: Statistische analyse trekproeven (Dutch) [Impact of clamping: Statistical analysis pull-out experiments]. Technical Report H4134, Delft Hydraulics, Delft, URL <http://resolver.tudelft.nl/uuid:3ed22b31-84e5-46e3-a9c5-d7d66f38e9a7>.
- Coeveld, E.M., Knoeff, J.G., Bizarri, A., Klein Breteler, M., 2005. Residual strength of dike after failure of cover layer. In: Coastal Engineering 2004. World Scientific Publishing Company, pp. 3494–3506. http://dx.doi.org/10.1142/9789812701916_0282.
- De Vroeg, J., 1992. Reststerkte van dijkbekledingen (Dutch) [Residual strength of dike revetments]. Technical Report H195/H1490, Delft, URL <http://resolver.tudelft.nl/uuid:bd8e08e-4fbf-40eb-a5c-ab4ae2b77eed>.
- Duits, M., 2020. Hydra-NL v2.8 Gebruikershandleiding (Dutch) [Hydra-NL v2.8 Users manual]. Technical Report PR4315.10, HKV Lijn in Water.
- Eysink, W.D., Klein Breteler, M., 2003. Deltagootonderzoek naar stabiliteit van basalt (Dutch) [Delta flume research on the stability of basalt]. Technical Report H4327, Delft Hydraulics, Delft, URL <http://resolver.tudelft.nl/uuid:5511501c-8046-48c8-b078-b8ff51d76e46>.
- Flikweert, J.J., 2003. TR-25 Technisch Rapport Steenzettingen (Dutch) [TR-25b Technical report pattern-placed revetments]. Technical Report, TAW/ENW, ISBN: 90-369-5551-3. URL <http://resolver.tudelft.nl/uuid:ba7269ef-abfa-48c4-a477-4d46539ced5>.
- Flikweert, J.J., Akkerman, G.J., 2005. Onderzoeksprogramma Kennisleemtes Steenbekledingen (Dutch) [Knowledge gaps related to pattern-placed revetments]. Technical Report, Royal Haskoning, Nijmegen, URL <http://resolver.tudelft.nl/uuid:4881f4cf-7ab1-424a-95b8-8435181f0834>.
- Frissen, C.M., Bakker, H.L., Klein Breteler, M., 2002. Strength of placed block revetments on dikes determined from field tests. In: Finite Elements in Civil Engineering Applications: Proceedings of the Third Diana World Conference. Tokyo, Japan, 9–11 October 2002, CRC Press, pp. 304–310. <http://dx.doi.org/10.1201/9781003211365>, ISBN: 9781003211365.
- Gier, F., Schuttrumpf, H., Monnich, J., Van der Meer, J.W., Kudella, M., Rubin, H., 2012. Stability of interlocked pattern placed block revetments. Coastal Eng. Proc. 1 (33), 46. <http://dx.doi.org/10.9753/icce.v33.structures.46>.
- Herman, J., Usher, W., 2017. SALib: An open-source python library for sensitivity analysis. J. Open Source Softw. 2 (9), <http://dx.doi.org/10.21105/joss.00097>.
- Het Waterschapshuis, 2019. Digigids. URL <http://digigids.hetwaterschapshuis.nl/>. (Online; Accessed 8 February 2021).
- Hofland, B., Klein Breteler, M., 2005. De nauwkeurigheid van Zsteen bij golfklappen (Dutch) [The accuracy of Zsteen during wave impacts]. Technical Report H4455, WL | Delft Hydraulics, Delft, URL <http://resolver.tudelft.nl/uuid:289d1e3c-4670-4147-8684-fbde700ba18e>.
- Holcim Coastal, 2018. Basalton standard. URL <https://holcimcoastal.nl/>. (Online; Accessed 25 July 2023).
- Holthuijsen, L.H., 2007. Waves in Oceanic and Coastal Waters. Cambridge University Press, Delft, <http://dx.doi.org/10.1017/CBO9780511618536>, ISBN: 978-0-521-12995-4.
- Jongejan, R., 2017. WBI2017 Code Calibration, Reliability-based code calibration and semi-probabilistic assessment rules for the WBI2017. Technical Report, Rijkswaterstaat.
- Kaste, D., Mourik, G.C., 2016. Stabiliteit van Basalton 30 STS+ steenzetting bij golfaanval (Dutch) [Stability of Basalton 30 STS+ under wave loading]. Technical Report 1208618-008-HYE-0005, Deltares, Delft, URL <http://resolver.tudelft.nl/uuid:e85e0d1d-0483-4c5d-845b-0a3ce4d0d252>.
- Klein Breteler, M., 1995. Design Manual for Pitched Slope Protection, vol. 155, Balkema A.A. Publishers, ISBN: 9781315140995.
- Klein Breteler, M., 2007. Black box model voor afschuiving bij steenzettingen (Dutch) [Black box model for shear in pattern-placed revetments]. Technical Report H4635, WL | Delft Hydraulics, Delft, URL <http://resolver.tudelft.nl/uuid:94b3c8ff-199c-4580-8c66-598c147726ab>.
- Klein Breteler, M., 2018. Onderhoudseisen voor steenbekledingen op dijken (Dutch) [Maintenance requirements for pattern-placed revetments on dikes]. Technical Report 11201769-000-HYE-0004, Deltares, Delft.
- Klein Breteler, M., Bezuijen, A., 1992. Simplified design method for block revetments. In: Coastal Structures and Breakwaters. pp. 423–436. <http://dx.doi.org/10.1680/csab.16729.0029>, ISBN: 0-7277-4006-7.
- Klein Breteler, M., Eysink, W.D., 2005. Langudursterkte van steenzettingen (Dutch) [Long-term strength of pattern-placed revetments]. Technical Report H4475, Delft Hydraulics, Delft, URL <http://resolver.tudelft.nl/uuid:efbdf47-997a-4437-b133-4bd57d05bf12>.
- Klein Breteler, M., Eysink, W.D., 2007. Reststerkte van steenzetting met zuilen na initiële schade (Dutch) [Residual strength of a pattern-placed revetment with initial damage]. Technical Report H4327, Delft Hydraulics, Delft, URL <http://resolver.tudelft.nl/uuid:ee8f1719-dc61-4a67-b4bc-71098169a25e>.
- Klein Breteler, M., Mourik, G.C., 2009. Gebruikershandleiding Steentoets2008: Onderzoeksprogramma Kennisleemtes Steenbekledingen (Dutch) [User Guide Steentoets2008]. Technical Report H4846, Deltares, Delft, URL <http://resolver.tudelft.nl/uuid:c828ce30-f850-4b00-b395-630a50f762dc>.
- Klein Breteler, M., Mourik, G.C., 2019. Documentatie SteenToets v19.1.1 (Dutch) [Documentation SteenToets v19.1.1]. Technical Report 11203721-002-GEO-0004, Deltares, Delft.
- Klein Breteler, M., Provoost, Y., van Steeg, P., Wolters, G., Kaste, D., Mourik, G., 2018. Stability comparison of 9 modern placed block revetment types for slope protections. Coastal Eng. Proc. (36), 75. <http://dx.doi.org/10.9753/icce.v36.papers.75>.
- Klein Breteler, M., Van der Werf, I., Wenneker, I., 2012. Kwantificering golfbelasting en invloed lange golven (Dutch) [Quantification of wave loading and the influence of long waves]. Technical Report 1204727-009-HYE-0007, Deltares, Delft, URL <http://resolver.tudelft.nl/uuid:507d7dc9-a544-44b5-bb84-22d26daa45a2>.
- Klerk, W.J., 2022. Decision on life-cycle reliability of flood defence systems (Ph.D. thesis). Delft University of Technology, Delft, <http://dx.doi.org/10.4233/uuid:877bed45-d775-40bb-bde2-d2322c3b34f0>, ISBN: 978-94-6384-313-3.
- Klerk, W.J., Kanning, W., Kok, M., Bronsveld, J., Wolfert, A.R.M., 2021. Accuracy of visual inspections of flood defences. Struct. Infrastruct. Eng. 19 (8), 1076–1090. <http://dx.doi.org/10.1080/15732479.2021.2001543>.
- Kroetz, H.M., Tessari, R.K., Beck, A.T., 2017. Performance of global metamodeling techniques in solution of structural reliability problems. Adv. Eng. Softw. 114, 394–404. <http://dx.doi.org/10.1016/j.advengsoft.2017.08.001>.
- Lind, N.C., 1995. A measure of vulnerability and damage tolerance. Reliab. Eng. Syst. Saf. 48 (1), 1–6. [http://dx.doi.org/10.1016/0951-8320\(95\)00007-0](http://dx.doi.org/10.1016/0951-8320(95)00007-0).
- Longuet-Higgins, M.S., 1952. On the statistical distribution of sea waves. J. Mar. Res. 11 (3), URL http://elischolar.library.yale.edu/journal_of_marine_research/774.
- Lubbers, C.L., Klein Breteler, M., 2000. Grootchalig modelonderzoek naar stabiliteit van taludbekledingen (Dutch) [Large-scale modeling study of stability of pattern-placed revetments]. Technical Report H1550, WL | Delft Hydraulics, Delft, URL <http://resolver.tudelft.nl/uuid:30b25c61-6d16-4c80-8c08-8d4980751cb4>.
- Peters, D.J., 2007. Meet- en analyserapport proefnemingen op geklemde steenzettingen op dijken in Zeeland (Dutch) [Measurement and analysis report experiments conducted on pattern-placed revetments on dikes in Zeeland]. Technical Report 9R5069.A0, Royal Haskoning, Nijmegen, URL <http://resolver.tudelft.nl/uuid:f557c122-f443-4e9c-8342-6cea535d2866>.
- Peters, D.J., 2017. Design of pattern-placed Revetments (Ph.D. thesis). Delft University of Technology, Delft, <http://dx.doi.org/10.4233/uuid:0b67a0dd-a951-46f3-bbaa-86270e546c4e>, ISBN: 978-946-295-665-0.
- Pilarczyk, K.W., Klein Breteler, M., Bezuijen, A., 1995. Wave forces and structural response of placed block revetments. In: International Conference on Coastal Engineering 1995. American Society of Civil Engineers, URL <http://resolver.tudelft.nl/uuid:a34d8fc4-82e9-4b46-a889-cf4dfa1982ee>.
- Rijkswaterstaat, 2007. Voorschrift Toetsen op Veiligheid Primaire Waterkeringen (VTV2006) (Dutch) [Safety assessment guidelines for primary flood defenses (VTV2006)]. Technical Report, Rijkswaterstaat, Dienst Weg- en Waterbouwkunde, URL <http://resolver.tudelft.nl/uuid:15d29d22-862b-418e-903d-d90c01f04983>.
- Rijkswaterstaat, 2017. Website legal instruments for assessment of primary flood defenses (WBI 2017). URL <https://www.helpdeskwater.nl/secundaire-navigatie/english/water-and-safety/>.
- Saltelli, A., Ratto, M., 2008. Global Sensitivity Analysis. the Primer. John Wiley and Sons Ltd, <http://dx.doi.org/10.1002/9780470725184>, ISBN: 978-0-470-05997-5.
- Schierreck, G.J., Verhagen, H.J., 2019. Introduction To Bed, Bank and Shore Protection. Delft Academic Press, Delft, ISBN: 978-9065623089.
- Schoen, S., 2004. Onderzoek naar liggerwerking bij steenzettingen (Dutch) [Research into the beam behaviour of pattern-placed revetments]. Delft University of Technology, Delft, URL <http://resolver.tudelft.nl/uuid:6ca4854e-8086-456e-9ea0-190a6288837f>.
- Schüttrumpf, H.F.R., 2001. Wellenüberlaufströmung bei Seedeichen (German) [Overflow flow of waves in coastal dikes] (Ph.D. thesis). Technischen Universität Carolo-Wilhelmina, Braunschweig, <http://dx.doi.org/10.24355/dbbs.084-200511080100-46>.
- Stive, R.J.H., 1983. Parametrisch model van een golfklap als functie van de tijd (Dutch) [Parametric model of a wave impact as a function of time]. Technical Report, Waterloopkundig Laboratorium Delft.
- Tarantola, S., Gatelli, D., Mara, T.A., 2006. Random balance designs for the estimation of first order global sensitivity indices. Reliab. Eng. Syst. Saf. 91 (6), 717–727. <http://dx.doi.org/10.1016/j.res.2005.06.003>, URL <https://www.sciencedirect.com/science/article/pii/S0951832005001444>.
- Teixeira, R., Nogal, M., O'Connor, A., 2021. Adaptive approaches in metamodel-based reliability analysis: A review. Struct. Saf. 89, 102019. <http://dx.doi.org/10.1016/j.strusafe.2020.102019>.
- Van der Meer, M.T., Moens, M.R., 1990. Schadecatalogus Voor Dijkbekledingen. Waltman Delft, Delft, ISBN: 90-212-9501-6. URL <http://resolver.tudelft.nl/uuid:2a74ed25-ba28-4817-bc2d-42c556c9b7ba>.
- Van der Meer, M.T., Niemeijer, J., Post, W.J., Heemstra, J., 2004. Technisch rapport waterspanningen bij dijken waterkeringen (Dutch) [Technical report on water pressures in dikes]. Technical Report DWW-2004-057, TAW, URL <http://resolver.tudelft.nl/uuid:bf74eeaf-dc41-43fc-9c94-acd70f4a8340>.
- Van der Vegt, N., 2021. Impact of Damages on the Stability and Reliability of Pattern-Placed Revetments (Master's thesis). Delft University of Technology, Delft, URL <http://resolver.tudelft.nl/uuid:0c645a77-0517-4902-a72c-bce0fc963ea9>.

- Vrijling, J.K., Van der Horst, C., Hoof, P., van Gelder, P.H.A.J.M., 2001. The structural analysis of the block revetment on the Dutch dikes. In: *Proceedings of the Coastal Engineering Conference*, Vol. 3. American Society of Civil Engineers, United States, pp. 1991–2003. [http://dx.doi.org/10.1061/40549\(276\)156](http://dx.doi.org/10.1061/40549(276)156), ISBN: 0-7844-0549.
- Wolters, G., 2016. Stabiliteit van Basalton 30 STS steenzetting bij golfaanval (Dutch) [Stability of Basalton 30 STS under wave loading]. Technical Report 1208618-007-HYE-0008, Deltares, Delft, URL <http://resolver.tudelft.nl/uuid:1fc90d8c-811a-4f74-826e-e67abb68f44e>.
- Wolters, G., Klein Breteler, M., 2011. Reststerkte van een dijk met steenzetting op een kleilaag (Dutch) [Residual strength of a dike with a pattern-placed revetment on a clay layer]. Technical Report 1202122.002, Deltares, Delft, URL <http://resolver.tudelft.nl/uuid:d3ed6cb6-c896-4eb4-9fb3-d82302471740>.
- Wouters, J., 1993. Reststerkte van dijkbekledingen. Stabiliteit van steenzetting en klei-onderlaag (Dutch) [Residual strength of dike revetments. Stability of pattern-placed and clay sublayer.]. Technical Report H1550, Waterloopkundig Laboratorium, Delft, URL <http://resolver.tudelft.nl/uuid:74eccc77-7aa7-4a24-a01b-daa3686f1dda>.